

COPY
071

CASE FILE
COPY



NACA TN No. 1679

NATIONAL ADVISORY COMMITTEE FOR AERONAUTICS

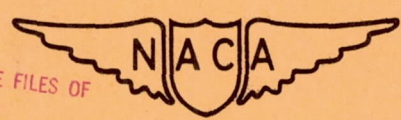
TECHNICAL NOTE

No. 1679

FLIGHT MEASUREMENTS OF THE LONGITUDINAL STABILITY, STALLING,
AND LIFT CHARACTERISTICS OF AN AIRPLANE HAVING A
35° SWEPTBACK WING WITHOUT SLOTS AND WITH
40-PERCENT-SPAN SLOTS AND A COMPARISON
WITH WIND-TUNNEL DATA

By S. A. Sjoberg and J. P. Reeder

Langley Aeronautical Laboratory
Langley Field, Va.



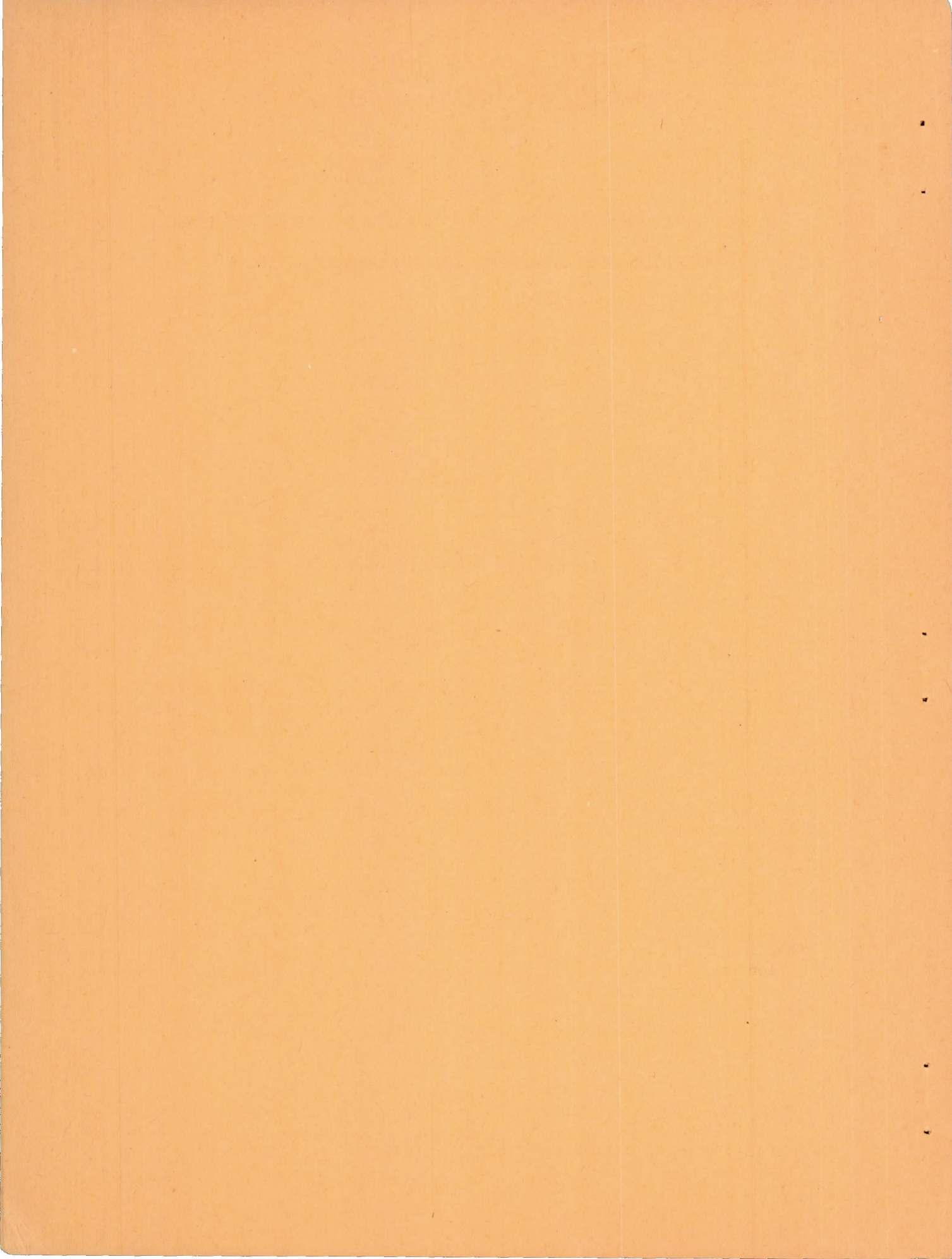
THIS DOCUMENT ON LOAN FROM THE FILES OF
NATIONAL ADVISORY COMMITTEE FOR AERONAUTICS
LANGLEY MEMORIAL AERONAUTICAL LABORATORY
LANGLEY FIELD, HAMPTON, VIRGINIA

Washington
August 1948

RETURN TO THE ABOVE ADDRESS.

REQUESTS FOR PUBLICATIONS SHOULD BE ADDRESSED
AS FOLLOWS:

NATIONAL ADVISORY COMMITTEE FOR AERONAUTICS
1724 F STREET, N.W.,
WASHINGTON 25, D.C.



NATIONAL ADVISORY COMMITTEE FOR AERONAUTICS

TECHNICAL NOTE No. 1679

FLIGHT MEASUREMENTS OF THE LONGITUDINAL STABILITY, STALLING,
AND LIFT CHARACTERISTICS OF AN AIRPLANE HAVING A
35° SWEEPBACK WING WITHOUT SLOTS AND WITH
40-PERCENT-SPAN SLOTS AND A COMPARISON
WITH WIND-TUNNEL DATA

By S. A. Sjoberg and J. P. Reeder

SUMMARY

Flight measurements were made at low speeds to determine the static longitudinal stability, stalling, and lift characteristics of an airplane having a wing swept back 35° at the quarter-chord line. The airplane was tested without slots on the wing and with slots which extended from 40 percent to 80 percent of the semispan of the sweptback-wing panels measured from the inboard end.

The longitudinal stability of the airplane with the flaps up was high with or without slots throughout the speed range tested. With the flaps down the longitudinal stability was high at moderate speeds, but near the stall the stability of the airplane was neutral or slightly negative. The pilot had no serious objections to the neutral longitudinal stability present near the stall because he could easily control pitching with the elevator. The slots increased the stalling speed and therefore reduced the speed range over which the neutral or slightly negative stability was present.

The stalling characteristics of the airplane without slots on the wing were objectionable. With the flaps up an uncontrollable rolling and pitching motion occurred, and the airplane reached extreme attitudes after the stall. With the flaps down the airplane both rolled and settled abruptly at the stall and a large decrease in altitude resulted before recovery could be made. The stalling characteristics of the airplane with slots on the wing were good. A diverging lateral and directional oscillation occurred at the stall from which recovery could be effected easily.

The flight values of maximum normal-force coefficient were usually higher than the wind-tunnel values, probably because of the higher flight Reynolds number. The increase in maximum normal-force coefficient resulting from flap deflection was considerably greater in flight than in the wind tunnel. For the wing without slots, deflecting the flaps

increased the maximum normal-force coefficient 0.3 in flight and only 0.07 in the wind tunnel; whereas, for the wing with 40-percent-span slots, the increase was 0.2 in flight and 0.04 in the tunnel. Higher maximum normal-force coefficients were obtained without slots on the wing than with slots. Tuft pictures indicated that the juncture of the inboard end of the slot with the wing caused premature separation on the wing just inboard of the slot. The lower maximum normal-force coefficients which occurred with slots are probably due to the premature stalling.

INTRODUCTION

In order to determine the effects of sweepback on the low-speed flying qualities of an airplane, flight tests are being conducted at the Langley Laboratory with an airplane having a wing swept back 35° at the quarter-chord line. This paper presents the static longitudinal stability, stalling, and lift characteristics for the test airplane without slots on the wing and also with slots extending along 40 percent of the span of the sweptback-wing panels. The results of an investigation made to determine the lateral and directional stability and control characteristics of the airplane with 40-percent-span slots have been reported in reference 1. A $\frac{1}{4.5}$ -scale model of the airplane was tested in the Langley 300 MPH 7- by 10-foot tunnel, and wherever possible a comparison of the flight and wind-tunnel measurements is included.

AIRPLANE

A three-view drawing of the test airplane is shown in figure 1 and general dimensions and characteristics are listed in table I. Figures 2 and 3 are photographs of the airplane.

The airplane was flown without slots on the wing and also with slots which extended from 40 to 80 percent of the semispan of the sweptback-wing panels measured from the inboard end. A cross section of the slot and the forward part of the wing in a plane normal to the wing leading edge is shown in figure 4. In addition, modified slots were used. The modified slots were shaped so that had they been retractable a smooth wing contour would have been maintained with the slots in the retracted position. The modifications to the standard slots are shown by the dashed lines in figure 4.

The nose gear of the airplane was retractable but the main landing gear could not be retracted. The variation of elevator angle with stick-grip position is shown in figure 5.

INSTRUMENTS

The following instruments were installed in the airplane:

NACA Instrument	Measured quantity
Timer	Time (for synchronizing all records)
Airspeed recorder	Airspeed
Control-position recorders	Aileron, rudder, and elevator positions
Control-force recorders	Stick and pedal forces
Sideslip-angle recorder and indicator	Sideslip angle
Recording accelerometer	Normal, longitudinal, and transverse accelerations
Angular-velocity recorders	Pitching, rolling, and yawing velocities
Angle-of-attack recorder	Angle of attack
16-millimeter cameras	Photographs of tufts on wing

The installations for measuring airspeed and sideslip are described in reference 1. Airspeed as used herein is calibrated airspeed, which corresponds to the reading of a standard Army-Navy airspeed meter connected to a pitot-static system free from position error.

Angle-of-attack measurements were made in flight by using a vane mounted on a boom 1 chord length ahead of the left wing tip. The difference between the angle of attack of the thrust axis and the vane-angle reading was determined in the wind tunnel for a geometrically similar arrangement on the wind-tunnel model. A tunnel-wall correction was also applied to the wind-tunnel vane-angle measurements. When the airplane was rolling, the angle measured by the vane included the helix angle of the wing tip. The data presented herein have not been corrected for rolling because they are generally presented for steady-flight conditions.

TESTS, RESULTS, AND DISCUSSION

The static longitudinal stability, stalling, and lift characteristics were measured without slots and with 40-percent-span slots on the wing. All tests were made with the engine idling. The main landing gear of the airplane was extended for all tests. The nose gear was extended for the flaps-down tests and retracted for the flaps-up tests. Difficulty was experienced in determining the amount of fuel consumed in flight and therefore the center-of-gravity locations given are believed accurate to only ± 0.7 percent mean aerodynamic chord.

Static Longitudinal Stability

The static longitudinal stability characteristics of the test airplane without slots were determined with the flaps up and down and with a center-of-gravity location of approximately 26 percent mean aerodynamic chord. Figures 6 and 7 show the variation of elevator angle, elevator-stick force, angle of attack of thrust axis, and side-slip angle with calibrated airspeed for the airplane with flaps up and flaps down, respectively. The variation of elevator angle required for trim with normal-force coefficient is presented in figure 8 for both the flaps-up and flaps-down conditions.

With the flaps up (figs. 6 and 8) both the stick-fixed and stick-free stability are high throughout the speed range tested. With the flaps down figure 8 shows the stick-fixed stability is high up to a normal-force coefficient of approximately 1.0. A large decrease in stability occurred at a normal-force coefficient of 1.0 and the stability was neutral or slightly negative near the maximum normal-force coefficient. Figure 7 shows the stick-free stability was also neutral or slightly negative near the stall.

The pilot had no serious objections to the neutral longitudinal stability present near the stall with the flaps down. The airplane tended to pitch up when the loss of stability occurred, but the pilot could easily control the pitching with the elevator. If the longitudinal stability had been low at moderate normal-force coefficients, the airplane would probably have been highly unstable near the stall. This condition would be very objectionable to the pilot. It was not possible to make tests with the center of gravity far enough rearward to have low longitudinal stability at moderate normal-force coefficients because of the relatively far-forward location of the main landing gear on the airplane.

Longitudinal stability measurements with 40-percent-span slots on the wing were made with center-of-gravity locations of approximately 20 and 26 percent mean aerodynamic chord. The variation of elevator angle and elevator stick force with calibrated airspeed is shown in

figure 9 for the flaps-up condition and in figure 10 for the flaps-down condition. Figures 11 and 12 show the variation of elevator angle required for trim with normal-force coefficient and figures 13 and 14 show the variation of elevator stick force divided by impact pressure with normal-force coefficient.

With the flaps up the addition of slots had a negligible effect on the longitudinal stability at normal-force coefficients less than 1.0. At normal-force coefficients greater than 1.0 a decrease in stability occurred with the slots on the wing and an increase in stability occurred without slots. With the flaps down and the center of gravity at approximately 26 percent mean aerodynamic chord (figs. 12 and 14) a large decrease in stability occurred at a normal-force coefficient of approximately 1.2. The neutral or slightly negative stability extended over a smaller normal-force coefficient or speed range with slots on the wing than without slots, partly because the maximum normal-force coefficient was lower with the 40-percent-span slots than without slots. The data in figures 9 to 14 are shown only for unstalled conditions of flight. Although the stability was neutral at speeds slightly greater than the stalling speed, after the stall had occurred the stability was again positive inasmuch as up elevator was required to keep the airplane from pitching down. The wind-tunnel measurements of longitudinal stability showed the same trends as the flight data since with the flaps up there was no decrease in stability near the stall, but with the flaps down instability was present over a small range of angles of attack near the stall. After the stall stable pitching tendencies were again present. With the flaps down and the center of gravity at approximately 20 percent mean aerodynamic chord, the reduction in stick-fixed stability near the stall was apparently not so great as that for the more rearward center-of-gravity position. (See fig. 12.) Any changes in stability which occur with change in normal-force coefficient should be independent of the center-of-gravity location. With the center of gravity forward, considerably greater up elevator deflections were required for trim near the stall. It is believed that a loss in elevator effectiveness occurred at the higher deflections, and this loss is probably the reason the loss in stability near the stall was not apparent from the curves of elevator angle against normal-force coefficient and speed for the forward center-of-gravity location.

Stalling Characteristics

A time history of a stall for the test airplane without slots on the wing and with the flaps up is shown in figure 15(a). Photographs of tufts on the wing at various times during the stall are shown in figure 15(b). Figures 16(a) and 16(b) present data for a stall with the flaps down. The tuft pictures shown in figures 15(b) and 16(b) were taken with cameras mounted above the canopy and show the outboard 80 percent of the span of the sweptback-wing panels. The white lines on the wing are located at intervals of 20 percent of the semispan of

the sweptback-wing panels. Cameras were also mounted on the tail to photograph tufts on the inboard part of the wing. These pictures are not shown, but the results obtained are discussed. Angle-of-attack measurements are not shown on the time histories when appreciable rolling, pitching, or yawing is present because the angle of attack does not define the flow under such unsteady conditions.

With the flaps up (fig. 15) lateral and directional unsteadiness provided stall warning. The pilot considered the lateral unsteadiness an undesirable type of stall warning because of the tendency for a wing to drop near the ground. At the stall the airplane rolled uncontrollably to the left and a pitching oscillation also occurred. The pilot objected to the stalling characteristics because of the uncontrollable rolling and because of the extreme attitudes which the airplane reached after the stall. The tuft pictures showed that the wing first stalled at the root on the rear part of the wing and as the angle of attack was increased the stall spread forward and outward on the left wing but not on the right wing. At 36.1 seconds a large part of the left wing is stalled and the right wing is unstalled. When the airplane is rolling to the left (36.7 sec) the increase in angle of attack on the left wing due to rolling causes it to stall completely and the right wing remains unstalled.

With the flaps down (fig. 16) the decrease in longitudinal stability near the stall was the only stall warning present. The pilot considered this type of stall warning undesirable. The wing stalled very abruptly, as is shown by the tuft pictures of figure 16(b). At 55.5 seconds the wing is unstalled, and only 1.2 seconds later at 56.7 seconds both the left and right wings are completely stalled. The tuft pictures of the inboard part of the wing showed that the wing did not first stall at the root as was the case with the flaps up. As shown in figure 16(a) an abrupt decrease in normal acceleration occurred at 56.4 seconds and was followed by rapid rolling motions. The pilot objected to the stalling characteristics because the airplane settled abruptly when the stall occurred and there was a large loss in altitude before recovery could be made.

Time histories of stalls with the 40-percent-span slots on the wing are shown in figures 17 and 18 for the flaps-up and flaps-down conditions, respectively.

With the 40-percent-span slots on the wing and with the flaps up or down, lateral unsteadiness preceded the stall as shown on the time histories by the small rolling velocities present before the stall occurred. When the stall did occur, a diverging lateral and directional oscillation resulted. The pilot had no objections to this oscillation since the motions were not violent and recovery could easily be made. Inspection of the sideslip-angle and rolling-velocity curves of figures 17 and 18 indicate that the dihedral effect of the wing was still positive beyond the stall since the airplane tended to roll to the right when left sideslip was present and to the left when right sideslip was present.

Figures 19 and 20 show photographs of tufts on the right wing during stalls with the flaps up and down, respectively. These photographs were not obtained during the same stalls for which the time histories are presented and therefore no time correlation with the time history is possible. The times listed beneath the pictures are included to give an idea of the rate at which the angle of attack was being increased. Also, for the flight in which the tuft pictures were obtained, the center of gravity of the airplane was at approximately 26 percent mean aerodynamic chord; whereas, for the flight in which the time histories shown in figures 17 and 18 were obtained, the center of gravity was at approximately 20 percent mean aerodynamic chord. Less up elevator deflection is required for trim with the more rearward center-of-gravity position and therefore at a given angle of attack of the airplane the normal-force coefficients listed with the tuft pictures will be slightly higher than the normal-force coefficients obtained at the same angle of attack in the time histories.

Figures 19 and 20 show the stall patterns to be quite similar with the flaps up or down. Outflow is present over the rear part of the wing before any stalling occurs. The wing first stalls just inboard of the slot and, therefore, the juncture of the slot with the wing may be causing premature separation. The slots are effective in preventing stalling since the part of the wing behind the slot remains unstalled at all times.

Flight measurements showed that the directional stability of the airplane became low near the stall. The lateral and directional oscillation which occurred at the stall is probably due to the low directional stability, the high dihedral, and the unsteadiness of the partially stalled wing.

Brief tests were made with the 40-percent-span slots modified as shown in figure 4. Time histories and tuft pictures obtained during stalls with the modified slots on the wing and with the flaps up and down are shown in figures 21 and 22.

Modifying the slots had no appreciable effects on the stalling characteristics of the airplane with the flaps either up or down. The tuft pictures, figures 21(b) and 22(b), show the stall patterns to be substantially the same as those for the original slots, figures 19 and 20.

Lift Characteristics

The flight measurements of the variation of normal-force coefficient with angle of attack of thrust axis are shown in figure 23 for the airplane without slots and in figure 24 for the airplane with 40-percent-span slots. The maximum normal-force coefficients presented are those reached before any appreciable uncontrolled-for motions of the airplane

due to stalling occurred. In some conditions higher normal-force coefficients were reached after uncontrolled-for motions had occurred (fig. 17), but these were not considered usable normal-force coefficients. Figures 23 and 24 also include wind-tunnel results for comparison with the flight data. The flight and wind-tunnel results with the flaps-down are not directly comparable because in the wind-tunnel tests the flap deflection was 45° and in flight the flap deflection was approximately 40° . For the tests with the 40-percent-span slots the wind-tunnel model differed from the airplane in that on the model the outboard end of the 40-percent-span slots was at the wing tip and on the airplane the outboard end of the slots was located 20 percent of the semispan of the sweptback-wing panels inboard of the wing tip.

For the wing without slots (fig. 23) and with the flaps up, the agreement between the flight and wind-tunnel data is excellent. With the flaps down, the slopes of the flight and tunnel curves are in good agreement but the curves are displaced approximately 1° . At least a part of the displacement of the curves can be accounted for by the greater flap deflection used in the wind tunnel. At high angles of attack the wind-tunnel curve has a peculiar shape which is probably due to the relatively low test Reynolds number.

With the 40-percent-span slots and with the flaps up (fig. 24) the slopes of the flight and wind-tunnel curves are in good agreement throughout most of the angle-of-attack range, but the curves are displaced approximately 1.5° . The flight and wind-tunnel values of maximum normal-force coefficient are approximately the same, but as previously mentioned higher values of maximum normal-force coefficient were obtained in flight after uncontrolled-for motions of the airplane due to stalling had occurred. In the flaps-down condition, the agreement of the flight and wind-tunnel results is fair. Again a part of the displacement of the curves is due to the greater flap deflection used in the wind-tunnel tests. The flight data were obtained at considerably higher Reynolds numbers than the wind-tunnel data, which probably accounts for the higher maximum normal-force coefficients which occurred in flight. Deflecting the flaps resulted in a considerably greater increase in maximum normal-force coefficient in flight than in the wind tunnel. For the wing without slots, deflecting the flaps increased the maximum normal-force coefficient approximately 0.3 in flight and only 0.07 in the wind tunnel; whereas, for the wing with 40-percent-span slots, the increase was 0.2 in flight and 0.04 in the tunnel.

In figure 25 the flight data of figures 23 and 24 are replotted to show a comparison of the lift curves for the airplane without slots and for the airplane with 40-percent-span slots. Data are presented for both the flaps-up and flaps-down conditions. When the slots were

installed on the wing the maximum normal-force coefficients were considerably reduced. The maximum normal-force coefficients $C_{N_{max}}$ for the various slot and flap arrangements are as follows:

Slots (percent span)	Flaps	$C_{N_{max}}$
0	Up	1.20
40	Up	1.11
0	Down	1.51
40	Down	1.29

Comparison of the tuft pictures for the flaps-up condition, figures 15(b) and 19, and for the flaps-down condition, figures 16(b) and 20, shows that stalling occurred on the wing with the 40-percent-span slots at a considerably lower angle of attack than on the wing without slots. Separation first occurred just inboard of the slot. The juncture of the inboard end of the slot and the wing probably caused premature stalling, which resulted in a reduction in maximum normal-force coefficient. The tuft pictures for the 40-percent-span-slot configuration, figures 19 and 20, also show that the part of the wing spanned by the slot remains unstalled at all times.

CONCLUSIONS

Flight measurements have been made at low speeds to determine the longitudinal stability, stalling, and lift characteristics of an airplane having a wing sweptback 35° at the quarter-chord line. Measurements were made without slots on the wing and with slots which extended from 40 percent to 80 percent of the semispan of the sweptback-wing panels measured from the inboard end. The conclusions reached are as follows:

1. The longitudinal stability of the airplane with the flaps up was high with or without slots throughout the speed range tested. With the flaps down the longitudinal stability was high at moderate speeds, but near the stall the stability of the airplane became neutral or slightly negative. The pilot had no serious objections to the neutral longitudinal stability present near the stall because he could easily control pitching with the elevator. The slots increased the stalling speed and therefore reduced the speed range over which the neutral or slightly negative stability was present.

2. The stalling characteristics of the airplane without slots on the wing were objectionable. With the flaps up an uncontrollable rolling and pitching motion occurred, and the airplane reached extreme attitudes after the stall. With the flaps down the airplane rolled and settled abruptly at the stall and a large decrease in altitude resulted before recovery could be made.

3. The stalling characteristics of the airplane with 40-percent-span slots on the wing were good. Lateral unsteadiness preceded the stall and at the stall a diverging lateral and directional oscillation occurred. The pilot had no objections to the oscillation since the motions were not violent and recovery could easily be made.

4. The flight values of maximum normal-force coefficient were in most cases higher than the wind-tunnel values, probably because the flight data were obtained at higher Reynolds numbers.

5. The increase in maximum normal-force coefficient resulting from flap deflection was considerably greater in flight than in the wind tunnel. For the wing without slots, deflecting the flaps increased the maximum normal-force coefficient approximately 0.3 in flight and only 0.07 in the wind tunnel; whereas, for the wing with 40-percent-span slots, the increase was approximately 0.2 in flight and 0.04 in the tunnel.

6. With the slots on the wing the maximum normal-force coefficients were considerably lower than without slots on the wing. Tuft pictures indicated that the juncture of the inboard end of the slot with the wing caused premature separation on the wing just inboard of the slot. The reduction in maximum normal-force coefficient which occurred with slots on the wing is probably due to this premature stalling.

Langley Aeronautical Laboratory
National Advisory Committee for Aeronautics
Langley Field, Va., April 16, 1948

REFERENCE

1. Sjoberg, S. A., and Reeder, J. P.: Flight Measurements of the Lateral and Directional Stability and Control Characteristics of an Airplane Having a 35° Sweptback Wing with 40-Percent-Span Slots and a Comparison with Wind-Tunnel Data. NACA TN No. 1511, 1948

TABLE I.- AIRPLANE DIMENSIONS AND CHARACTERISTICS

Engine	Allison V-1710
Propeller:	
Diameter, ft	10.375
Number of blades	3
Engine-propeller gear ratio	2.23
Normal gross weight, lb	8700
Wing:	
Span, ft	33.6
Area, sq ft	250
Incidence (root section), deg	1.3
Airfoil section (normal to leading edge)	
Root	Modified 66,2x-116(a=0.6)
Tip	Modified 66,2x-216(a=0.6)
Mean aerodynamic chord, in.	93.6
Leading edge M.A.C. (in. behind L.E. root chord)	39.3
Aspect ratio	4.51
Taper ratio	1.84:1.00
Dihedral, deg	0
Sweepback (quarter-chord line), deg	35
Plain sealed wing flaps:	
Total area, sq ft	12.52
Span (along hinge line, each), in.	77.4
Travel (no load on system), deg	45
Ailerons:	
Span (along hinge line, each), in.	105
Area (rearward of hinge center line, each), sq ft	6.51
Travel (no load on system), deg	±17
Horizontal tail:	
Span, in.	175
Total area, sq ft	46.53
Stabilizer area, sq ft	33.7
Total elevator area, sq ft	12.83
Elevator area (behind hinge line), sq ft	9.56
Distance elevator hinge line to L.E. of M.A.C., in.	240.9
Elevator travel (no load on system), deg	
Upward	35
Downward	15
Vertical tail:	
Height along hinge line, in.	78.87
Fin area (above horizontal tail), sq ft	13.47
Ventral fin area, sq ft	17.10
Total rudder area, sq ft	10.26
Rudder area (behind hinge line), sq ft	8.3
Distance rudder hinge line to L.E. of M.A.C., in.	263
Rudder travel (no load on system), deg	±30

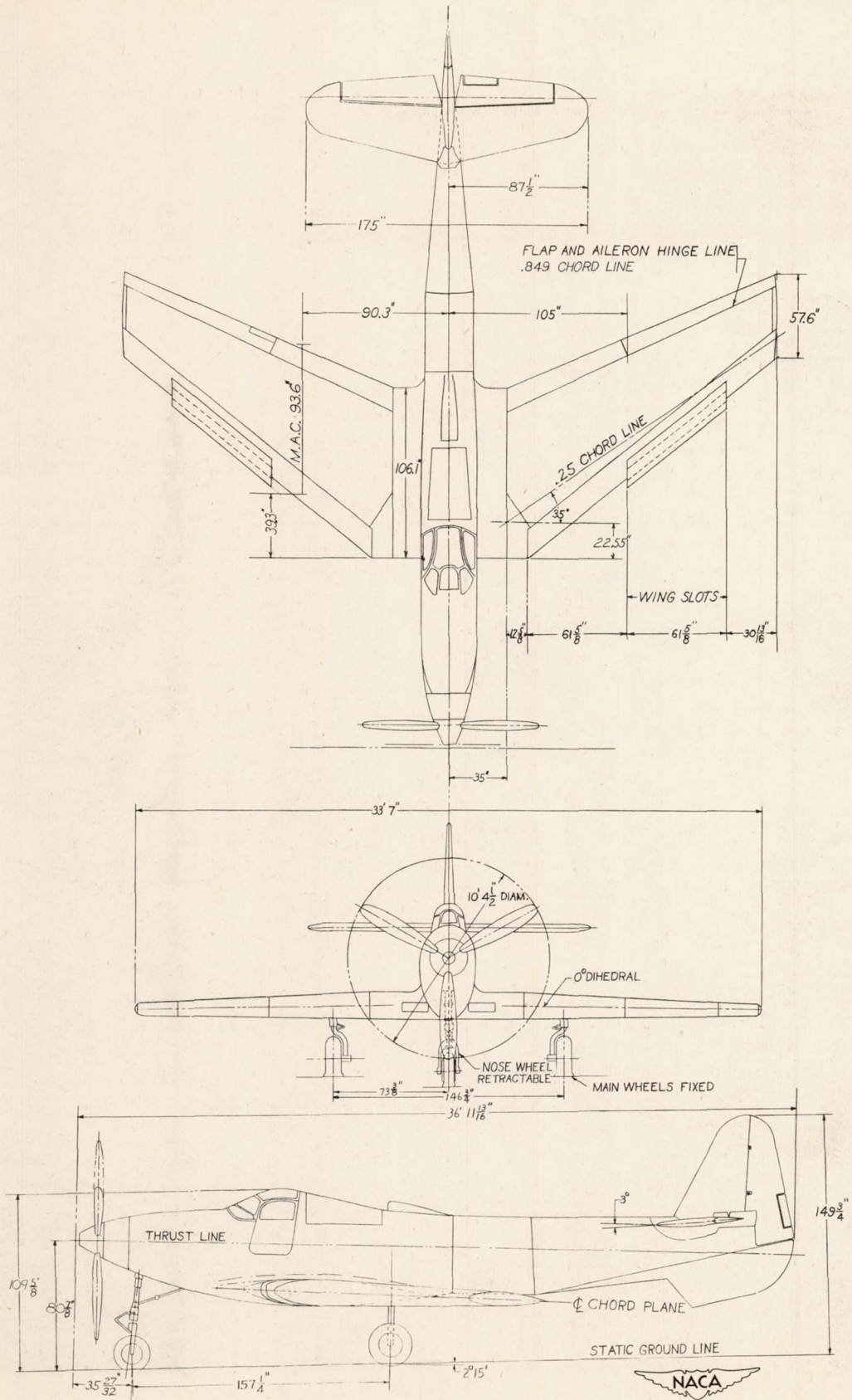
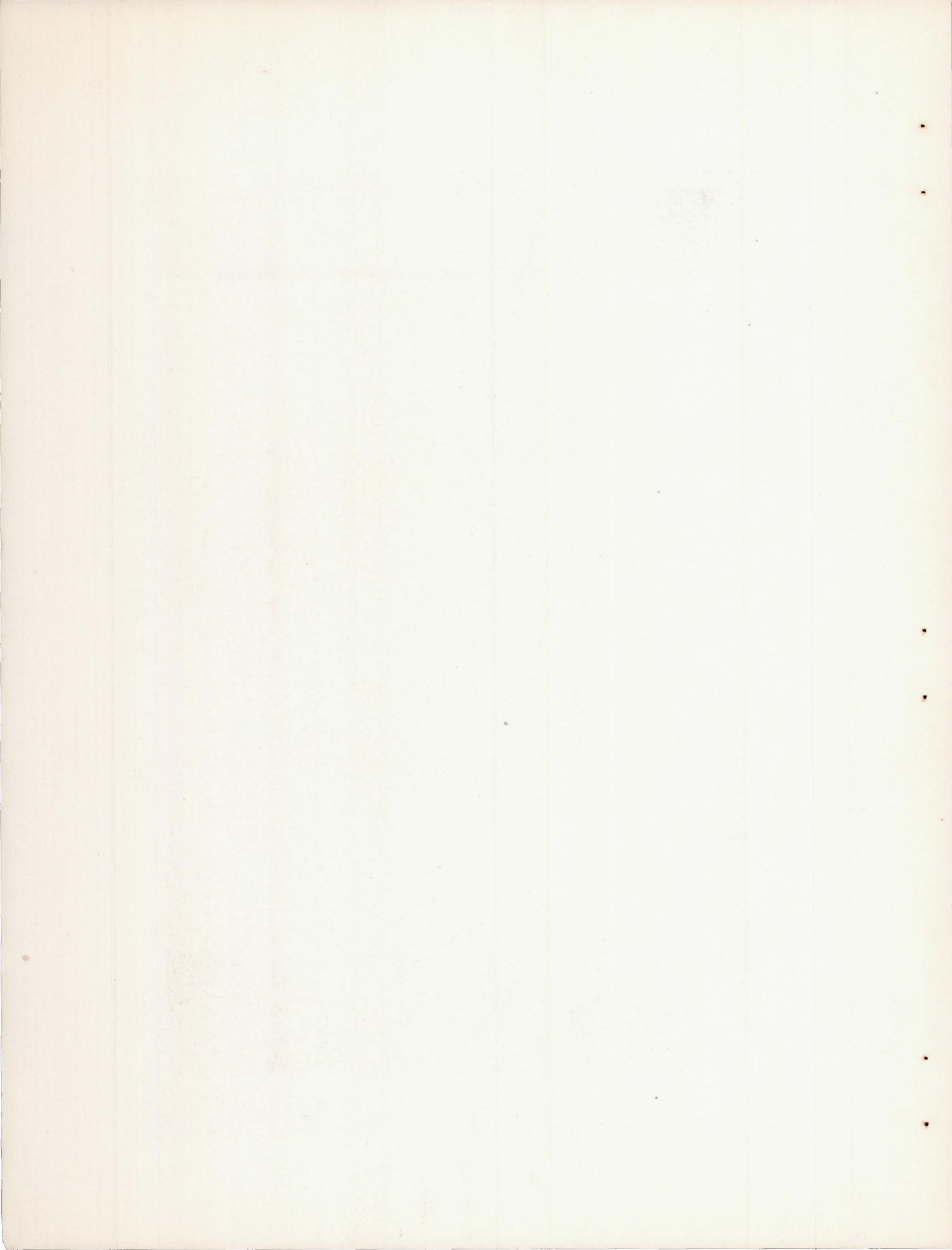


Figure 1.- Three-view drawing of test airplane.



Figure 2.- Front view of test airplane.



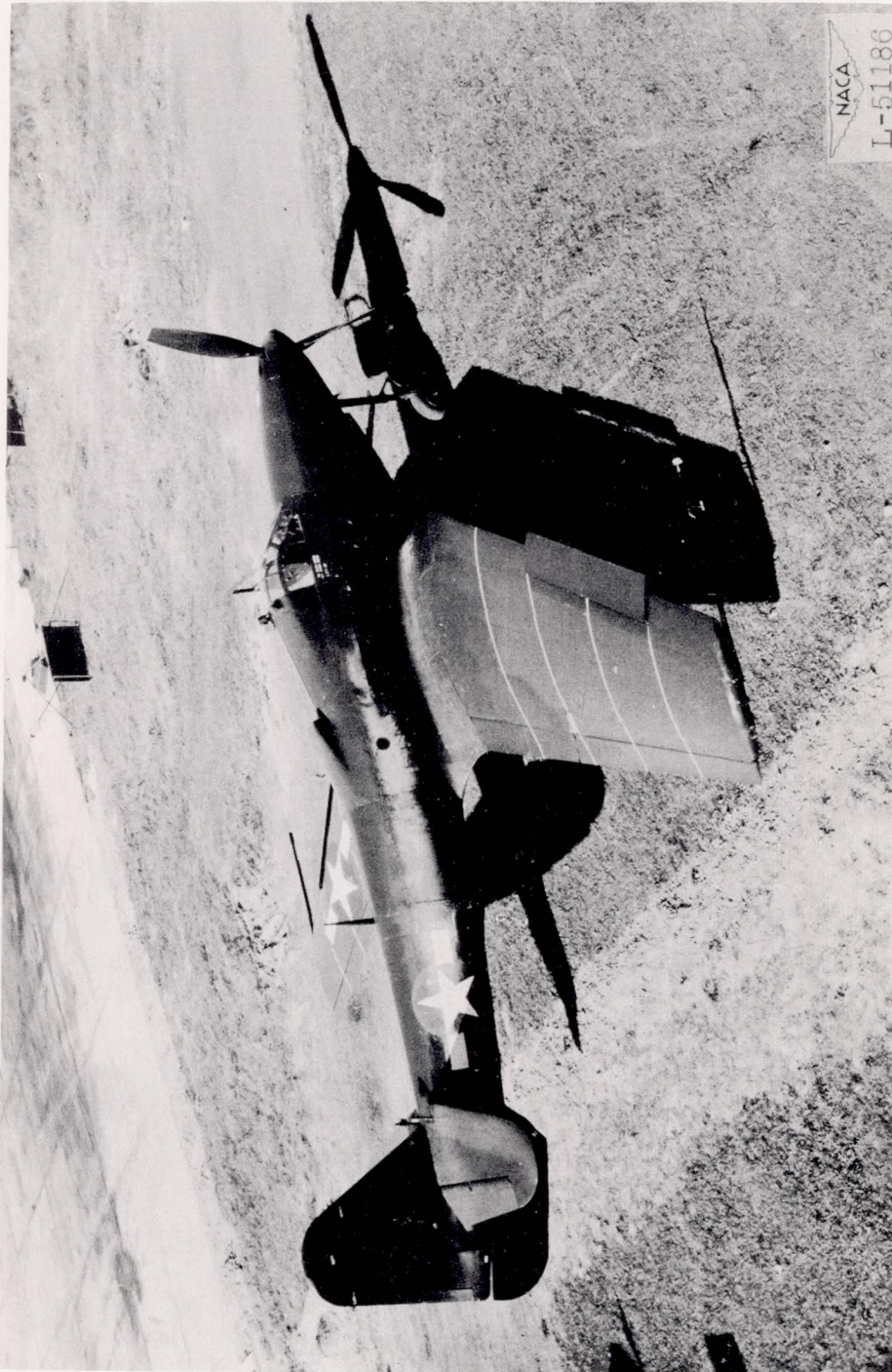
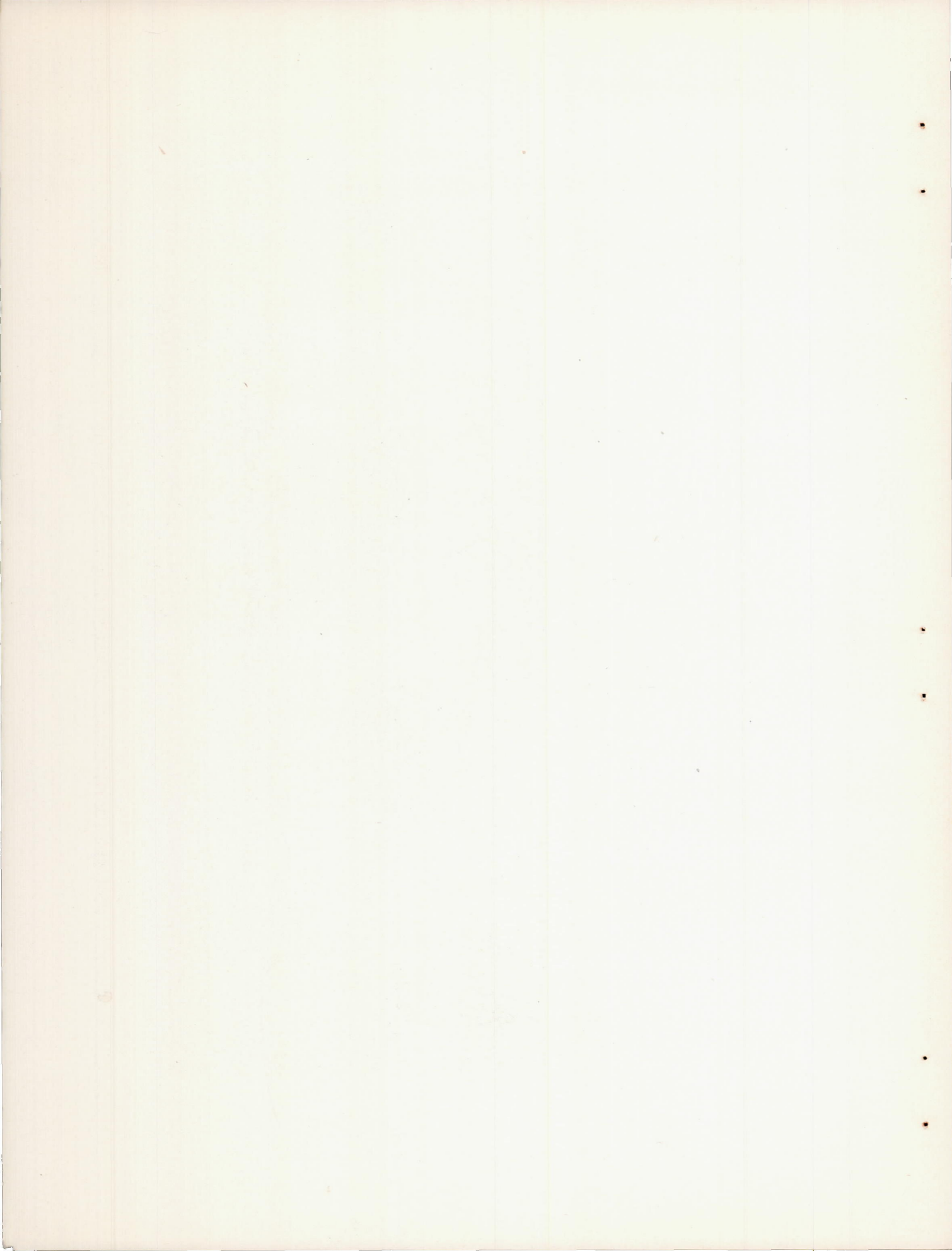
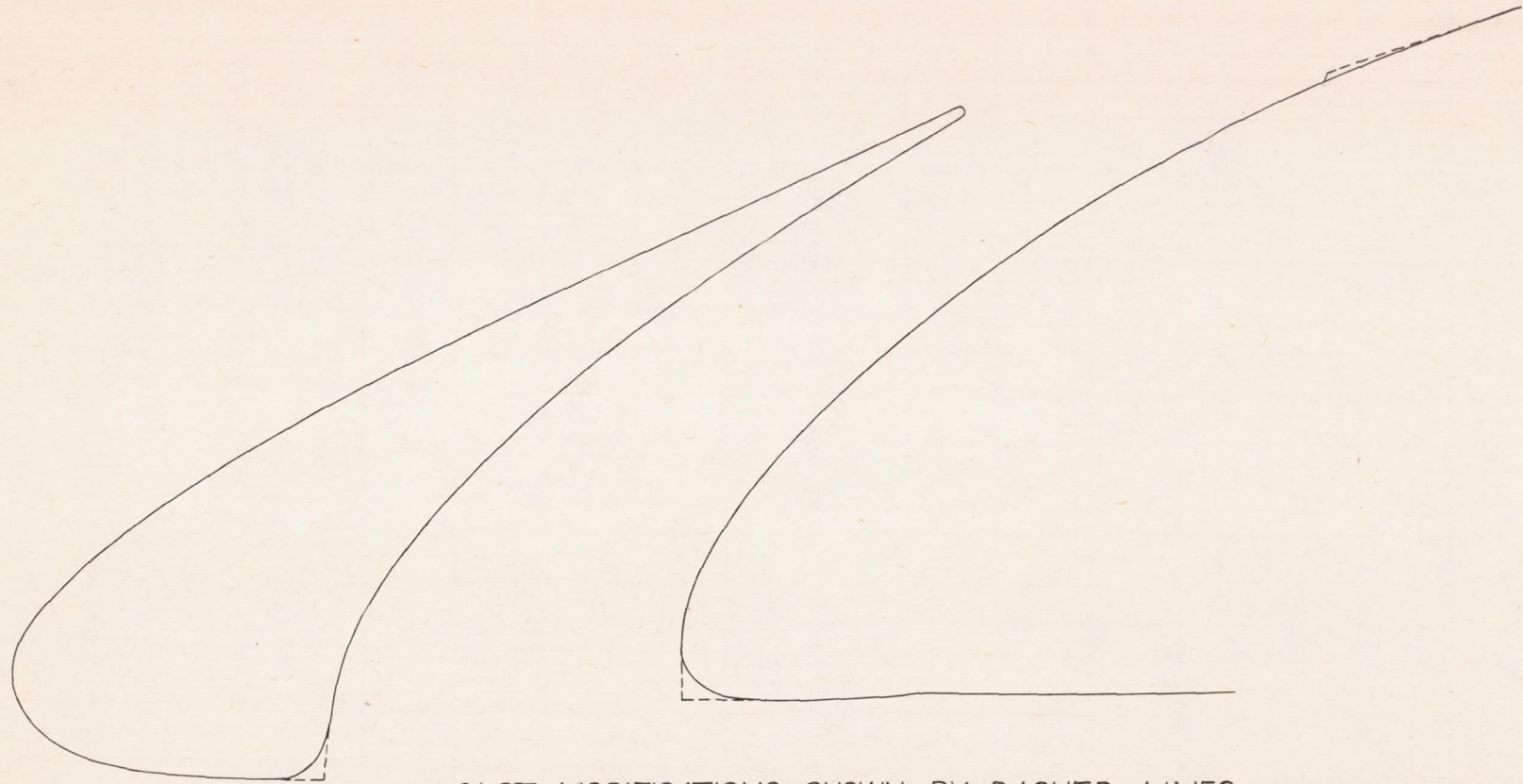


Figure 3.- Side view of test airplane.





SLOT MODIFICATIONS SHOWN BY DASHED LINES

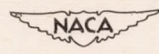
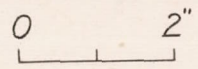


Figure 4.- Section of slot and forward part of wing in plane normal to wing leading edge.

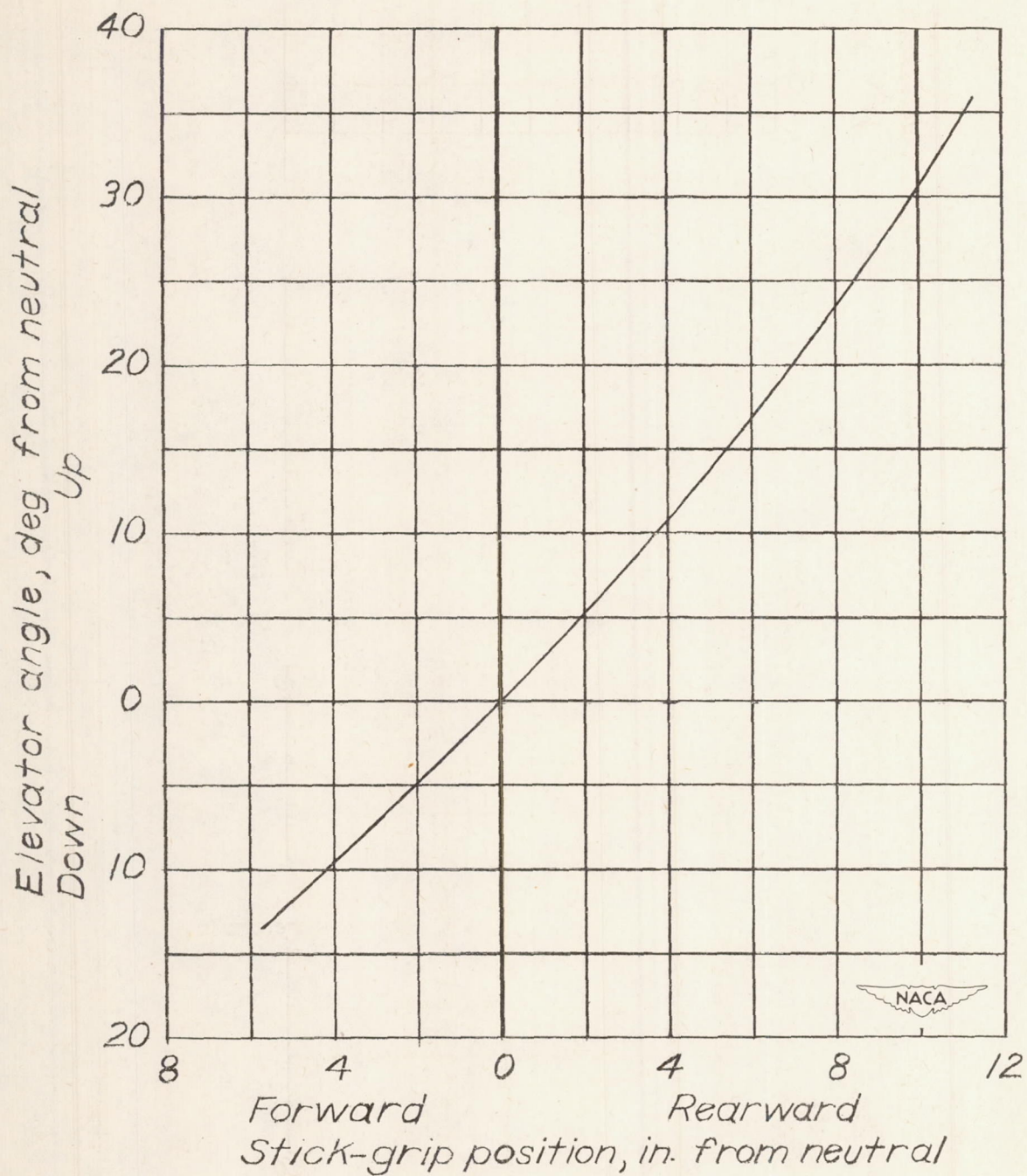


Figure 5.- Variation of elevator angle with stick-grip position. No load on system.

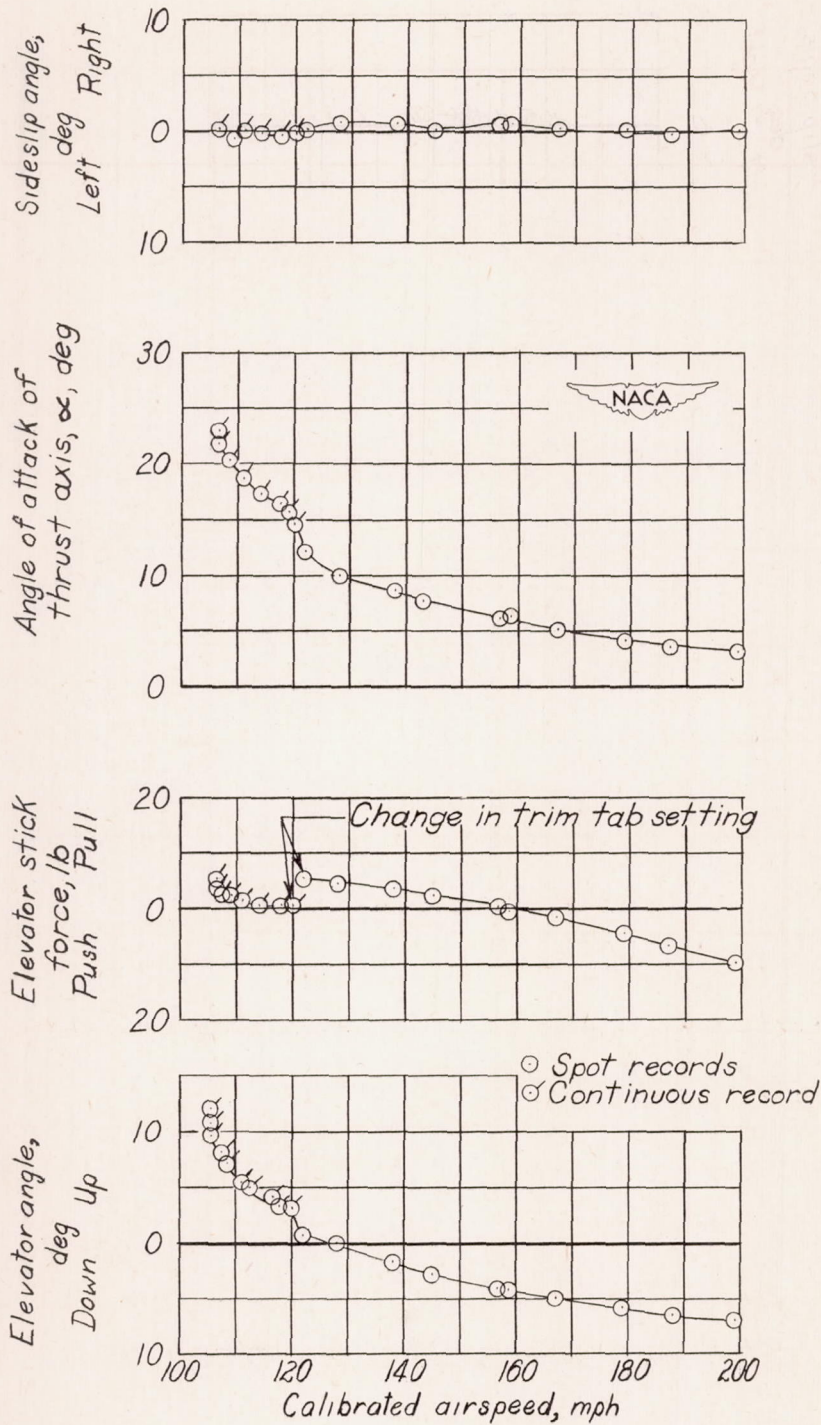


Figure 6.- Static longitudinal stability characteristics of test airplane without slots on wing. Flaps up; nose wheel up; engine idling; center of gravity at 26.3 percent mean aerodynamic chord.

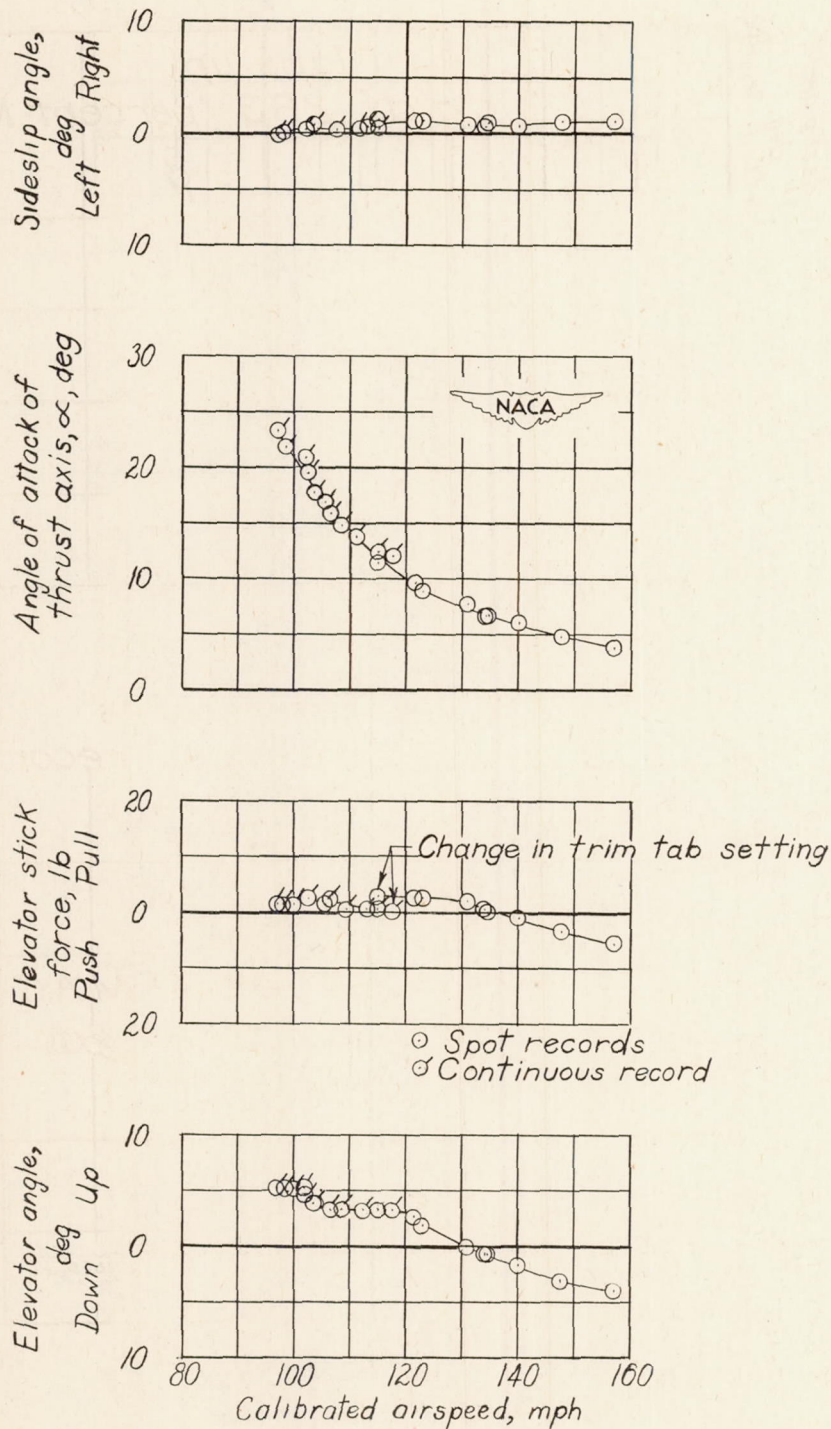


Figure 7.- Static longitudinal stability characteristics of test airplane without slots on wing. Flaps down; nose wheel down; engine idling; center of gravity at 26.4 percent mean aerodynamic chord.

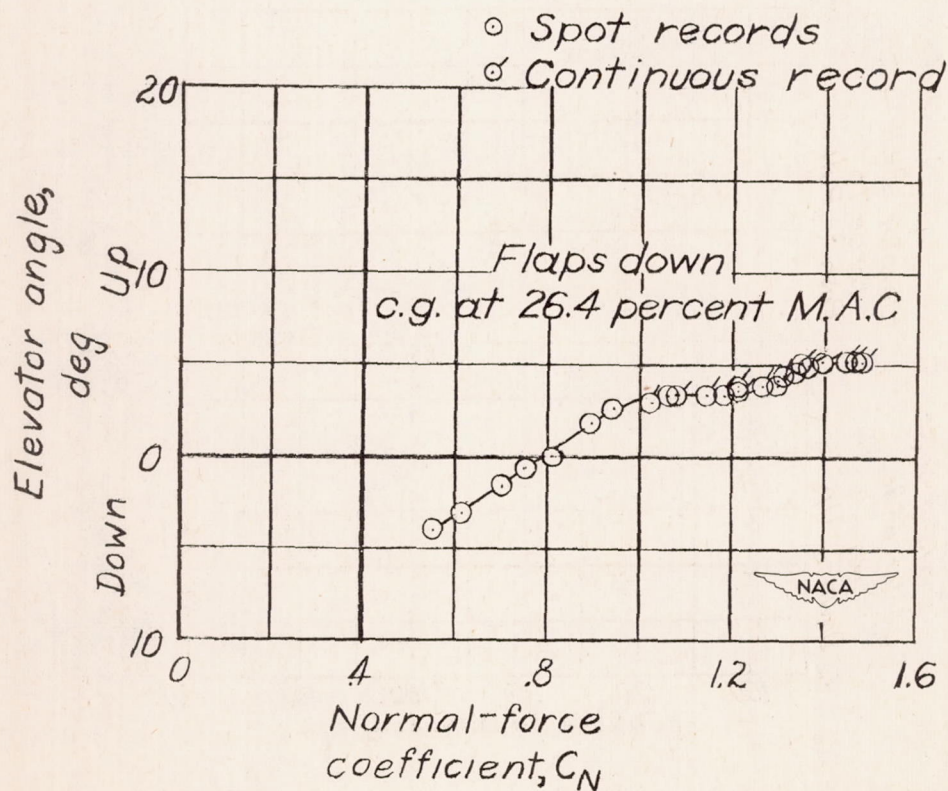
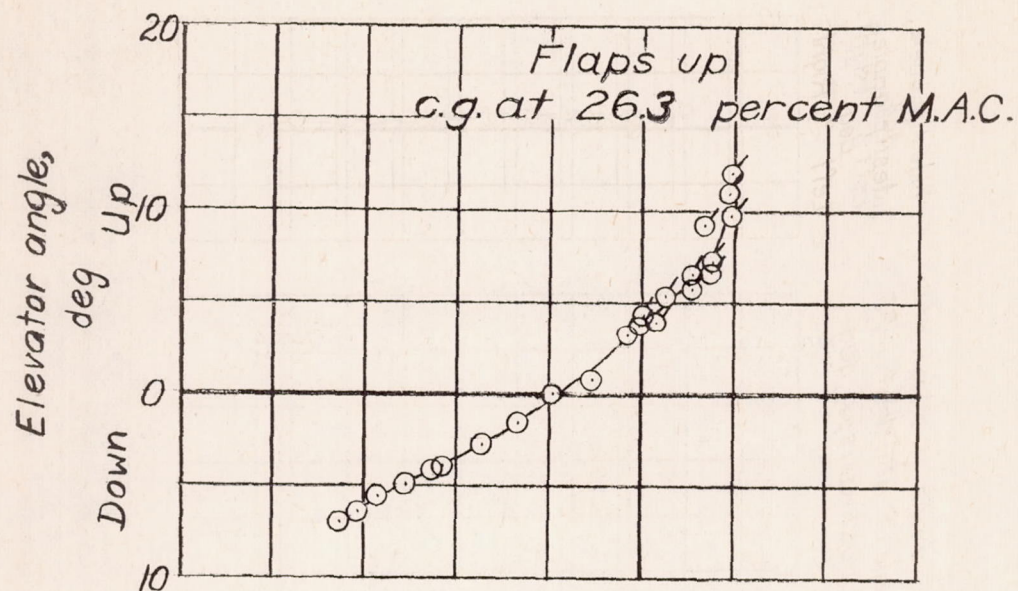
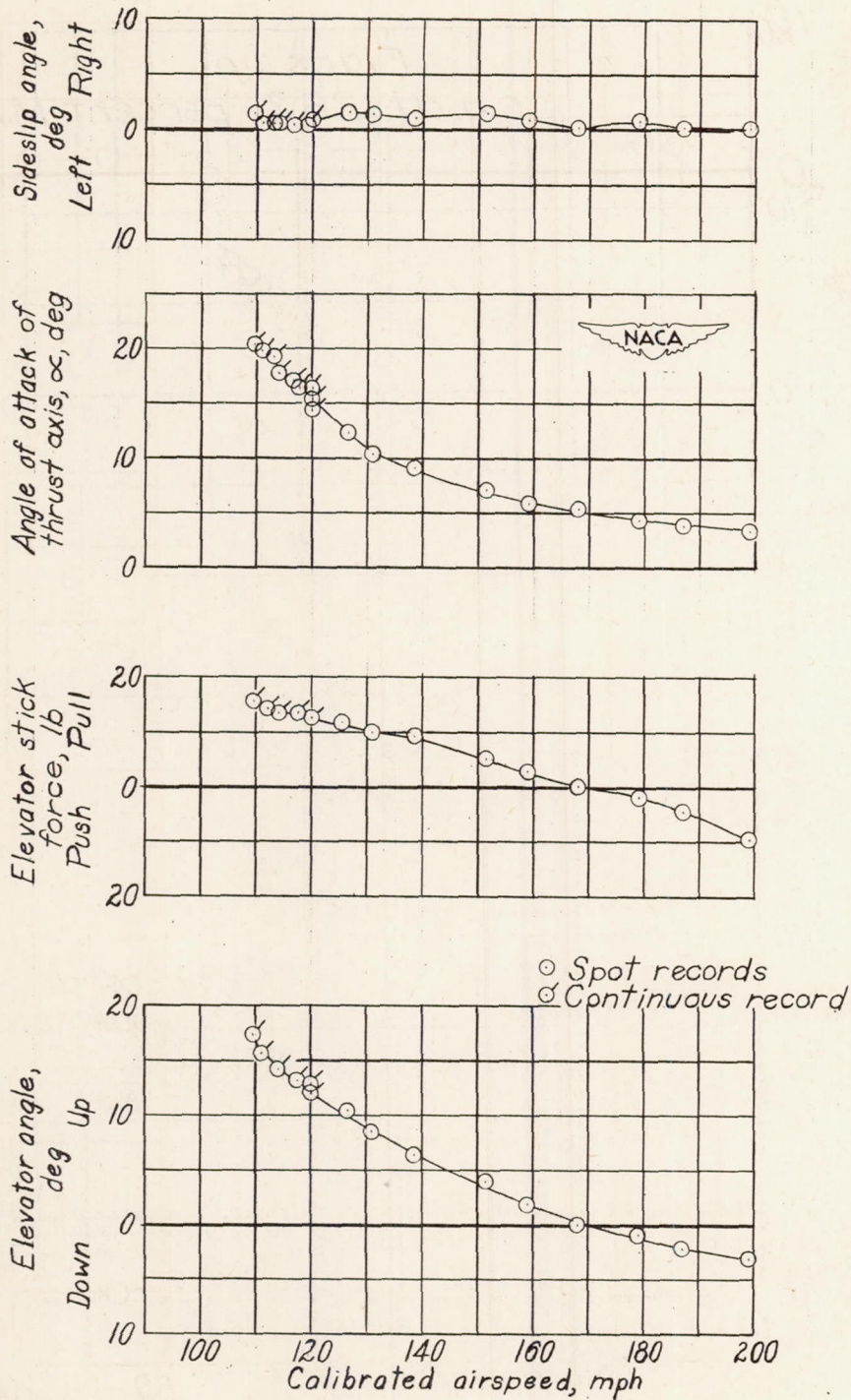
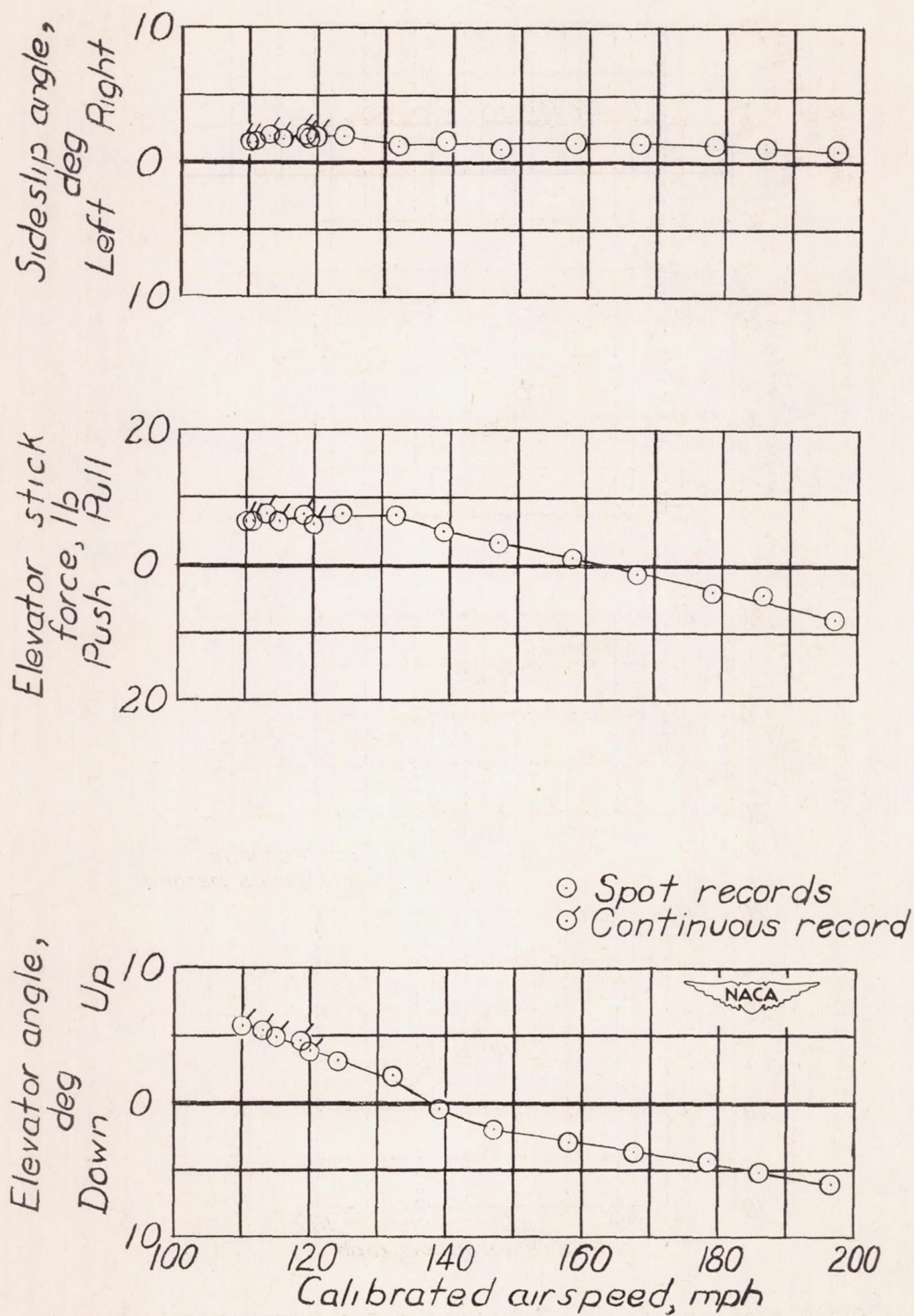


Figure 8.- Variation of elevator angle required for trim with normal-force coefficient for test airplane without slots on wing. Engine idling.



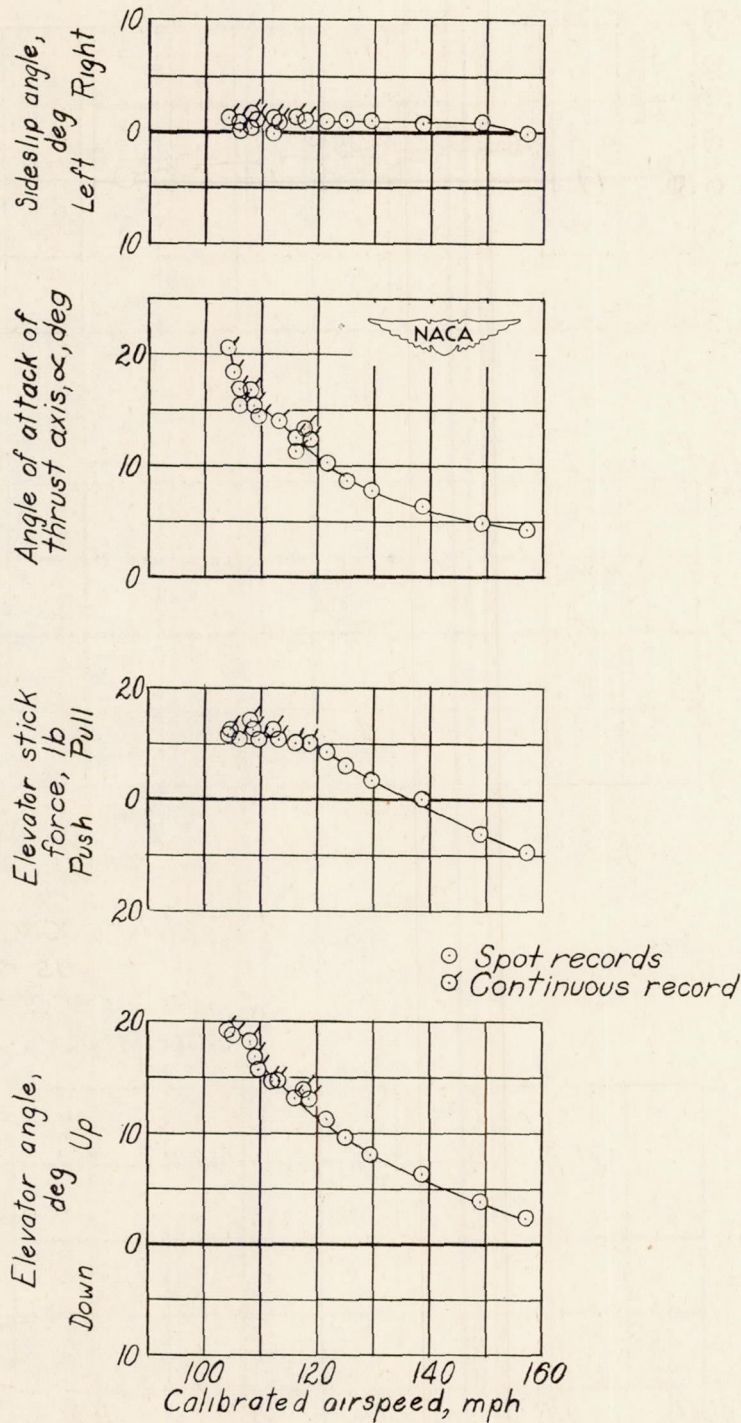
(a) Center of gravity at 20.6 percent mean aerodynamic chord.

Figure 9.- Static longitudinal stability characteristics of test airplane with 40-percent-span slots on wing. Flaps up; nose wheel up; engine idling.



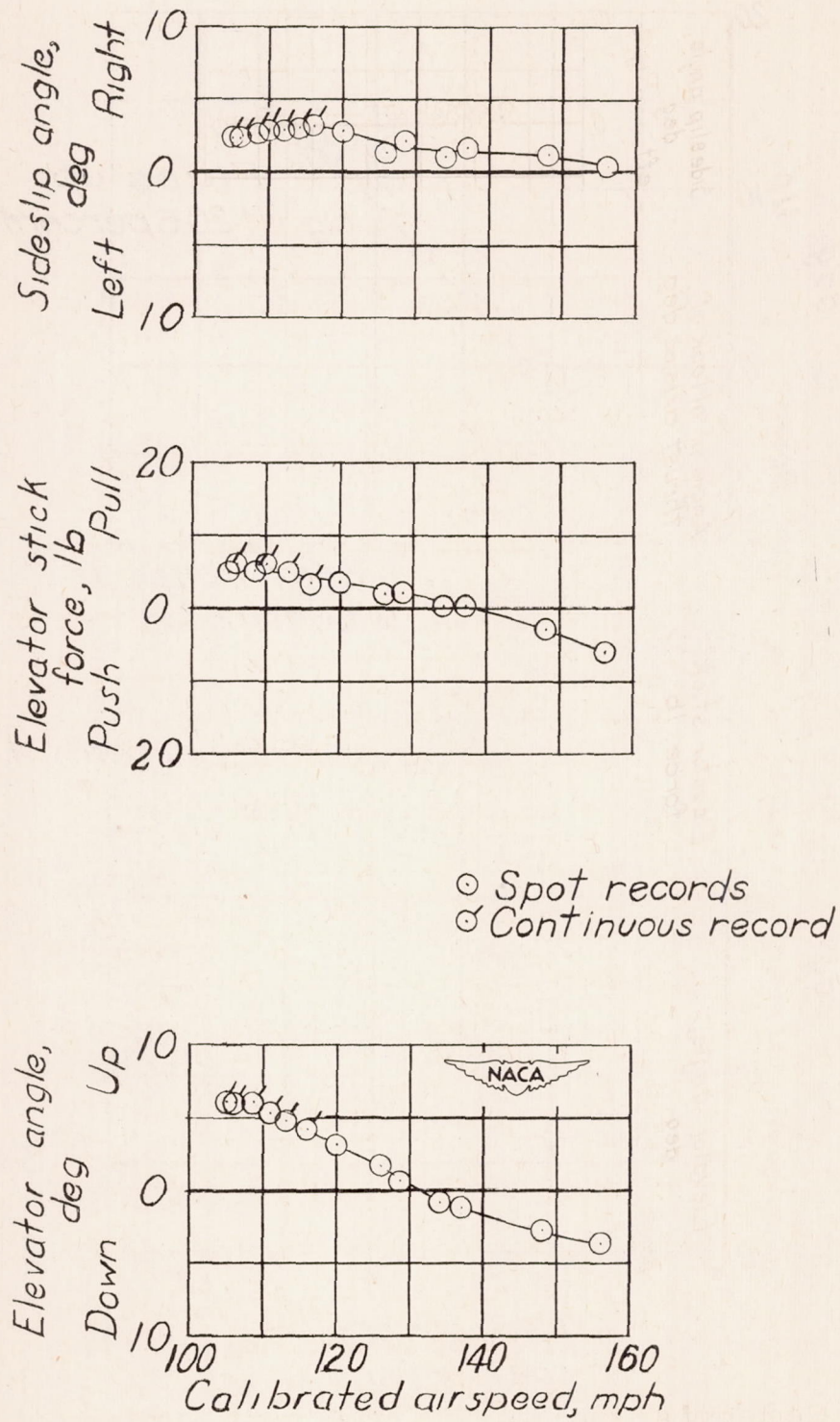
(b) Center of gravity at 26.2 percent mean aerodynamic chord.

Figure 9.- Concluded.



(a) Center of gravity at 20.3 percent mean aerodynamic chord.

Figure 10.- Static longitudinal stability characteristics of test airplane with 40-percent-span slots on wing. Flaps down; nose wheel down; engine idling.



(b) Center of gravity at 26.5 percent mean aerodynamic chord.

Figure 10.- Concluded.

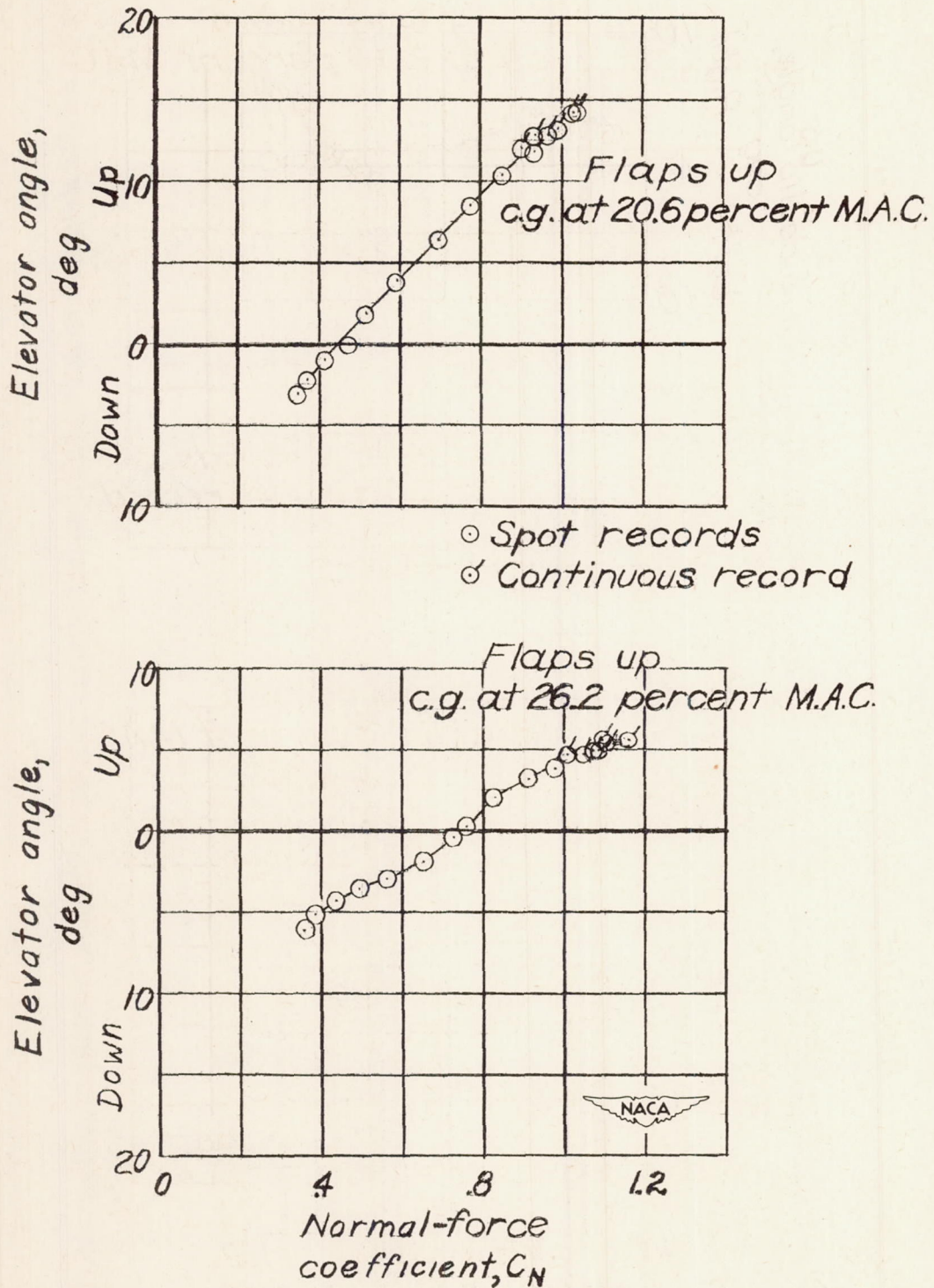


Figure 11.- Variation of elevator angle required for trim with normal-force coefficient for test airplane with 40-percent-span slots on wing. Flaps up; nose wheel up; engine idling.

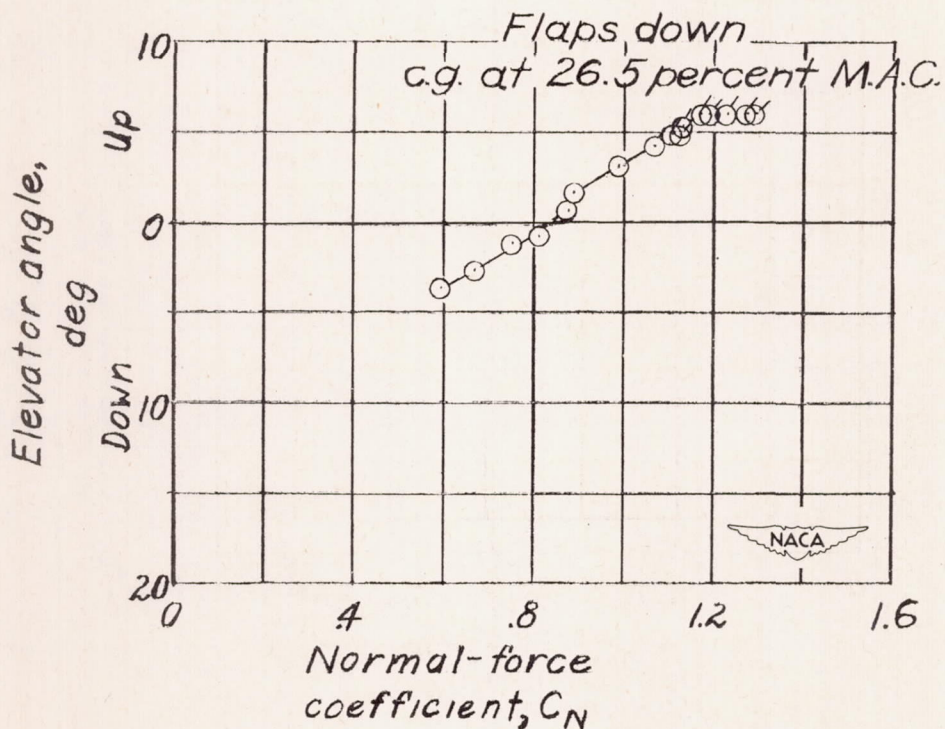
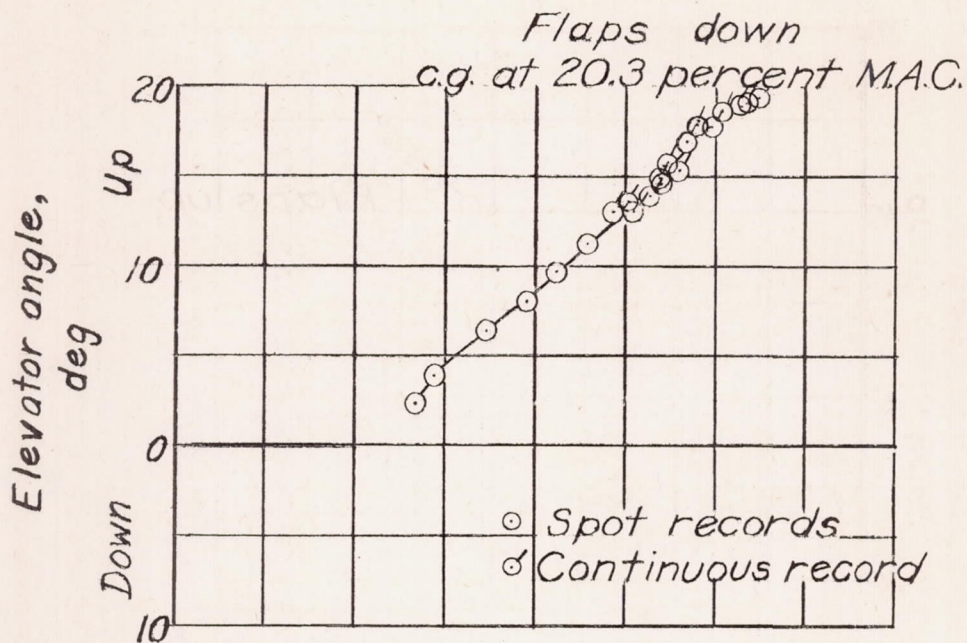


Figure 12.- Variation of elevator angle required for trim with normal-force coefficient for test airplane with 40-percent-span slots on wing. Flaps down; nose wheel down; engine idling.

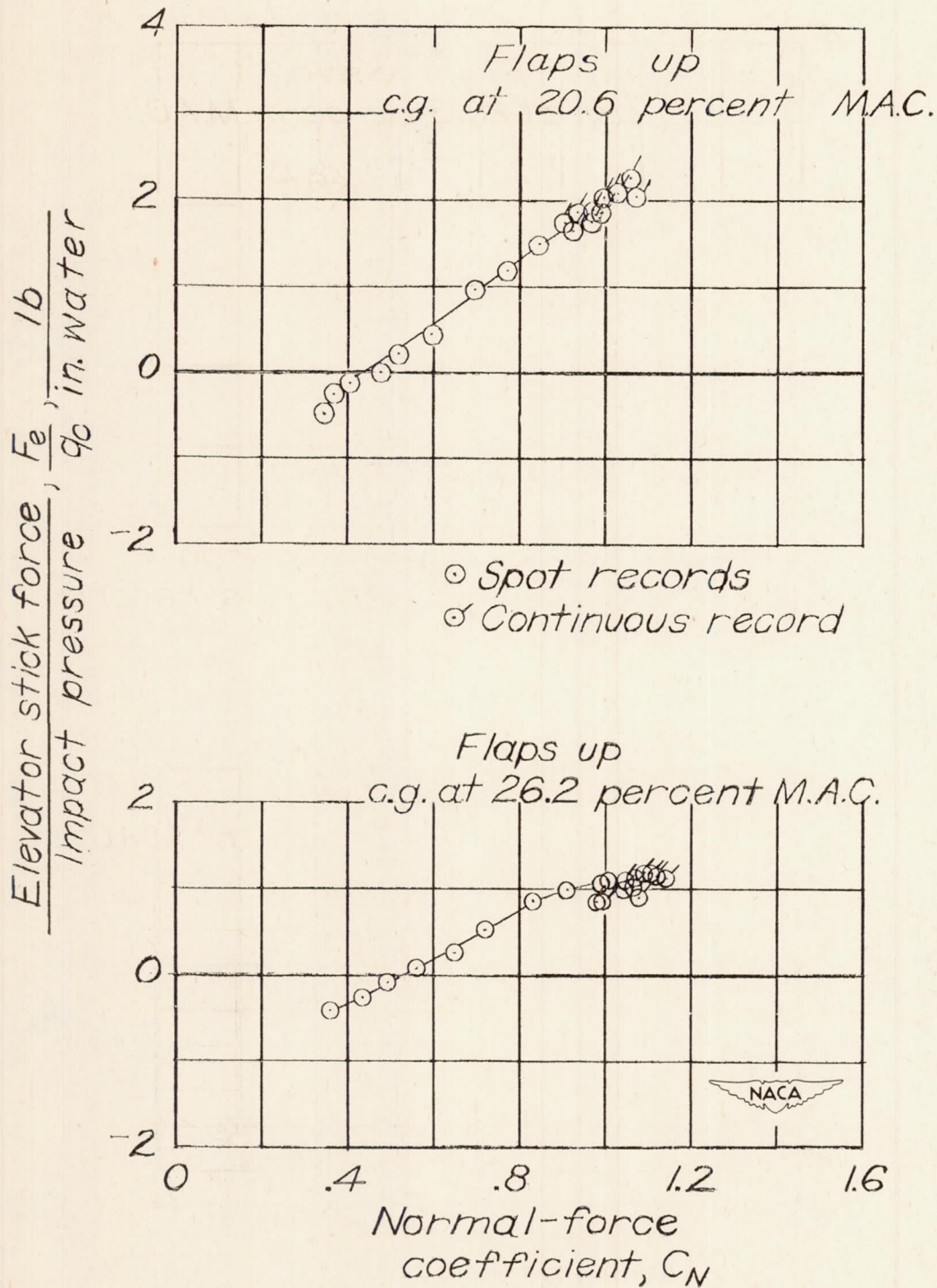


Figure 13.- Variation of elevator stick force divided by impact pressure with normal-force coefficient for test airplane with 40-percent-span slots on wing. Flaps up; nose wheel up; engine idling.

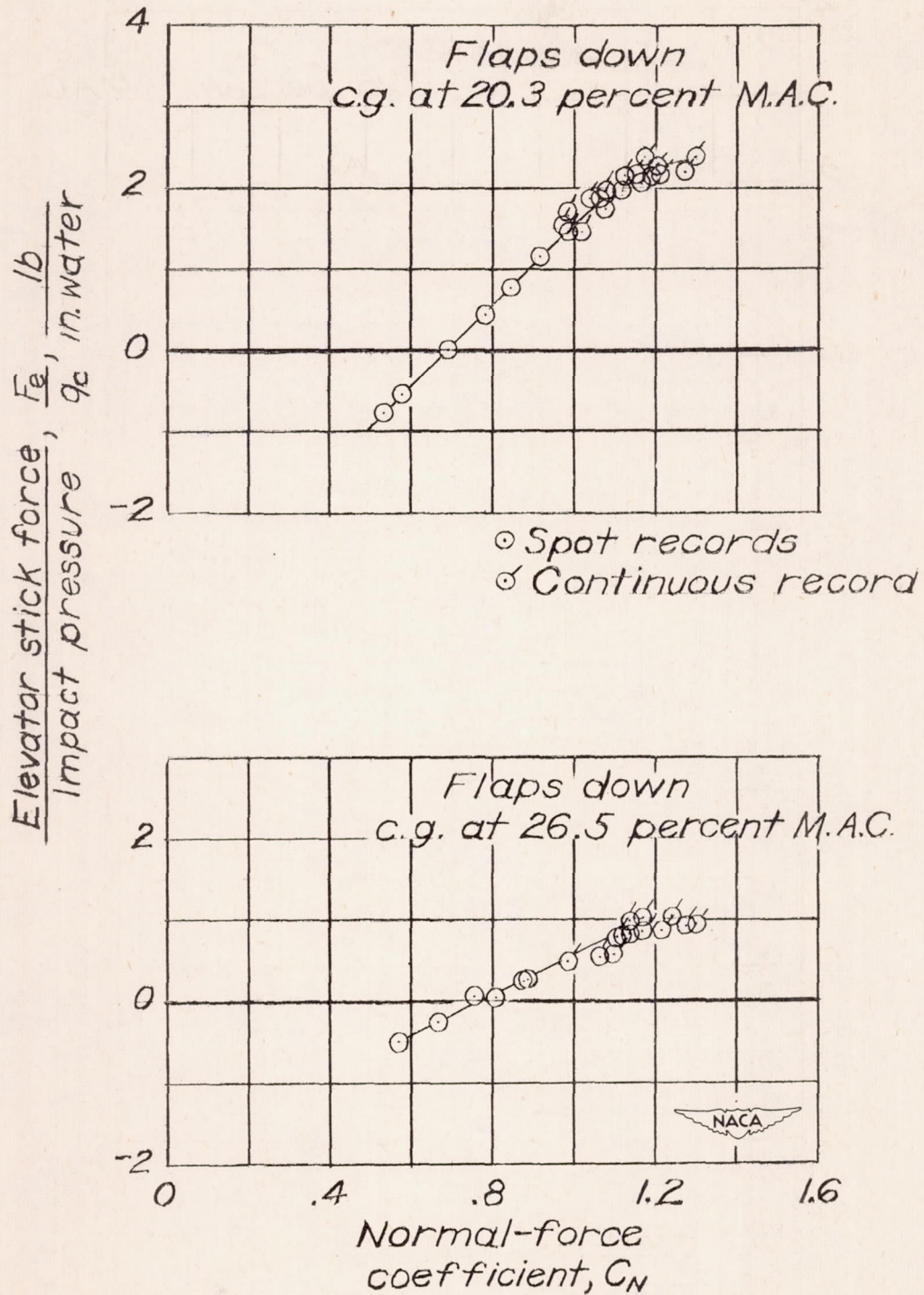
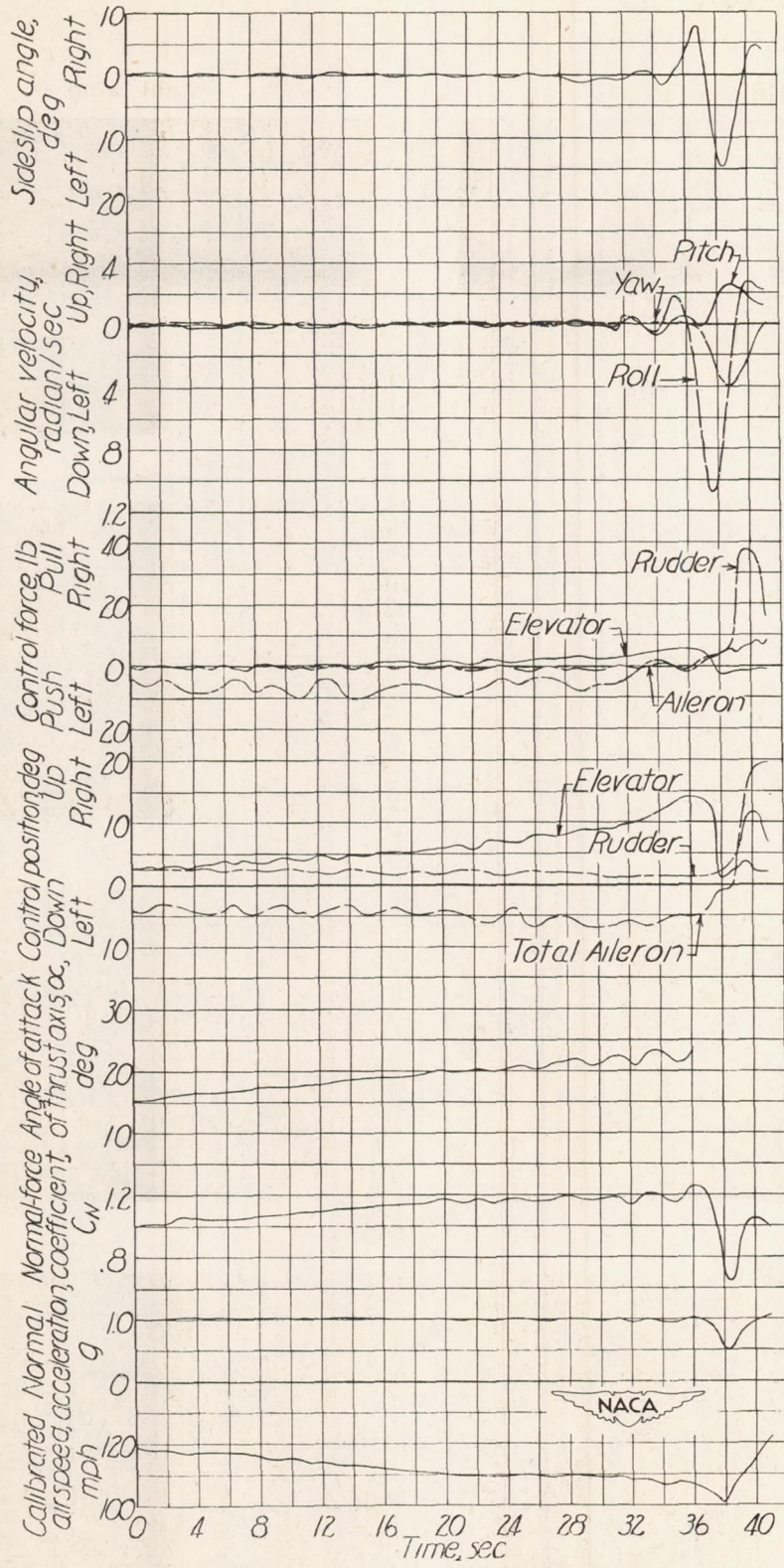


Figure 14.- Variation of elevator stick force divided by impact pressure with normal-force coefficient for test airplane with 40-percent-span slots on wing. Flaps down; nose wheel down; engine idling.

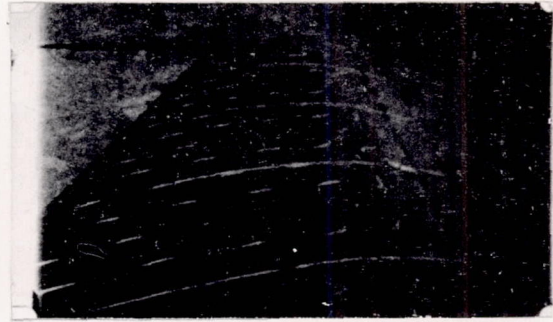
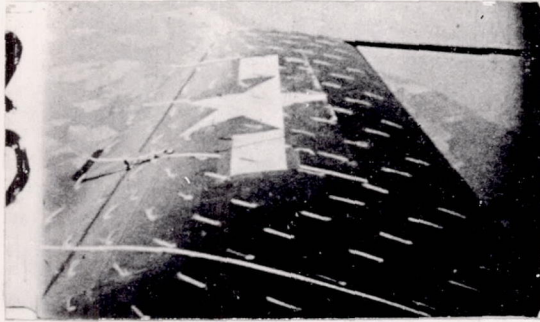


(a) Time history.

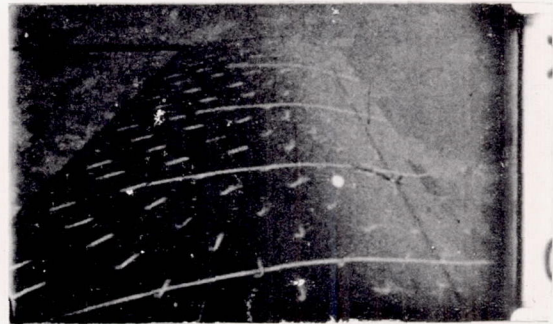
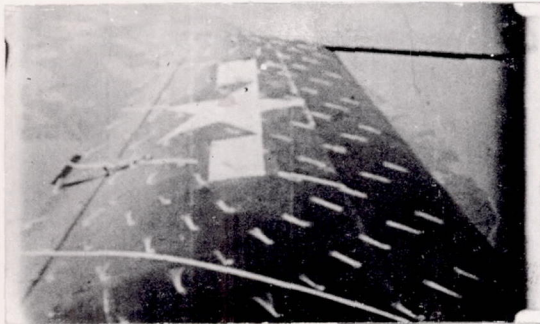
Figure 15.- Stall data for test airplane without slots on wing. Flaps up; nose wheel up; engine idling; center of gravity at 26.7 percent mean aerodynamic chord.

Left wing

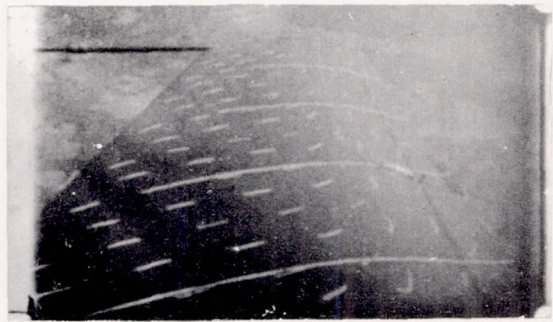
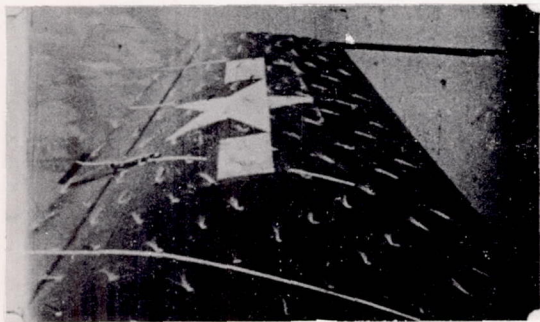
Right wing



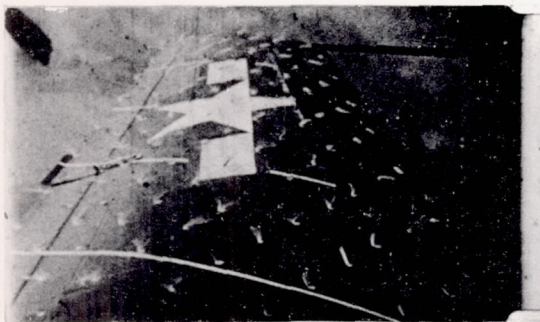
20.0 sec, $C_N = 1.17$, $\alpha = 20.0^\circ$



33.5 sec, $C_N = 1.21$, $\alpha = 23.3^\circ$



36.1 sec, $C_N = 1.26$, $\alpha = 23.6^\circ$



36.7 sec, $C_N = 1.23$

(b) Tuft pictures.

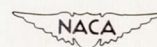
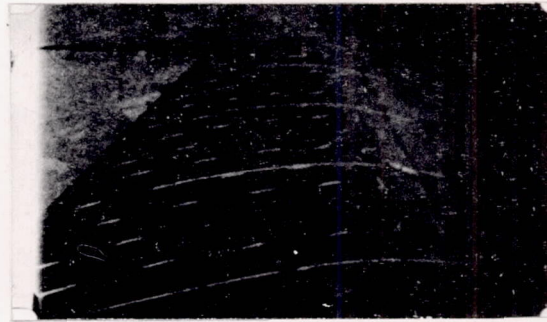
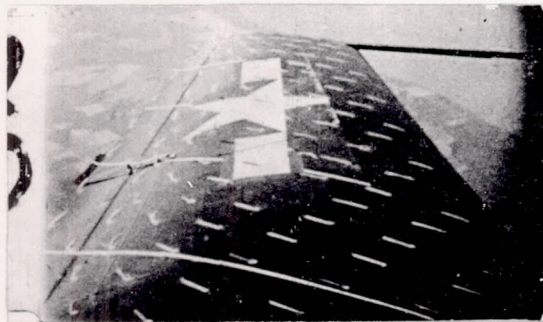


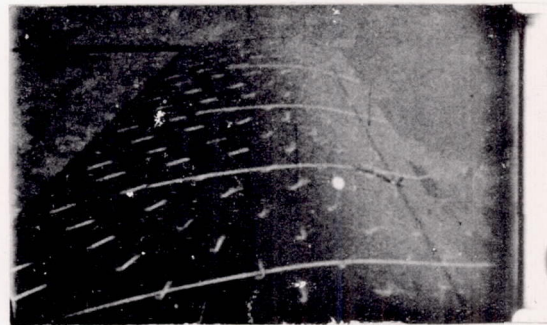
Figure 15.- Concluded.

Left wing

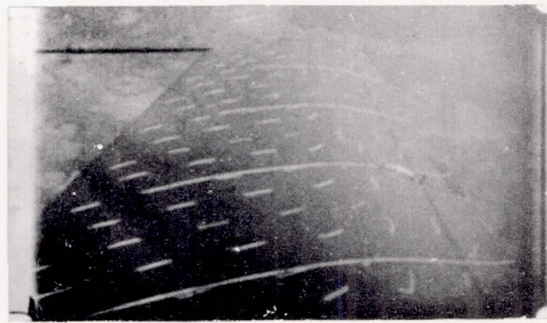
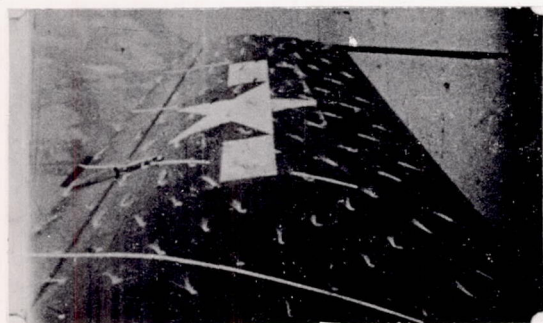
Right wing



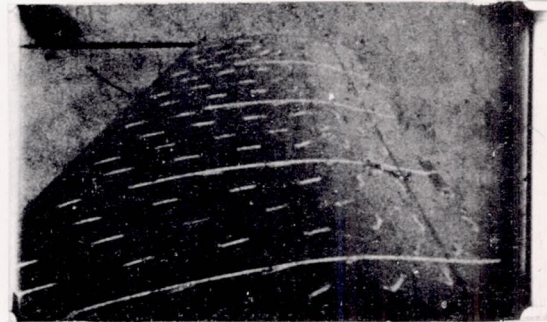
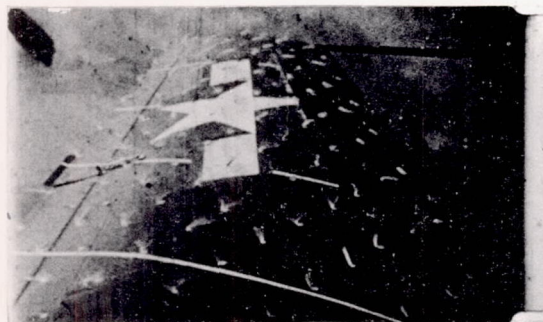
20.0 sec, $C_N = 1.17$, $\alpha = 20.0^\circ$



33.5 sec, $C_N = 1.21$, $\alpha = 23.3^\circ$



36.1 sec, $C_N = 1.26$, $\alpha = 23.6^\circ$



36.7 sec, $C_N = 1.23$

(b) Tuft pictures.

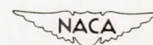
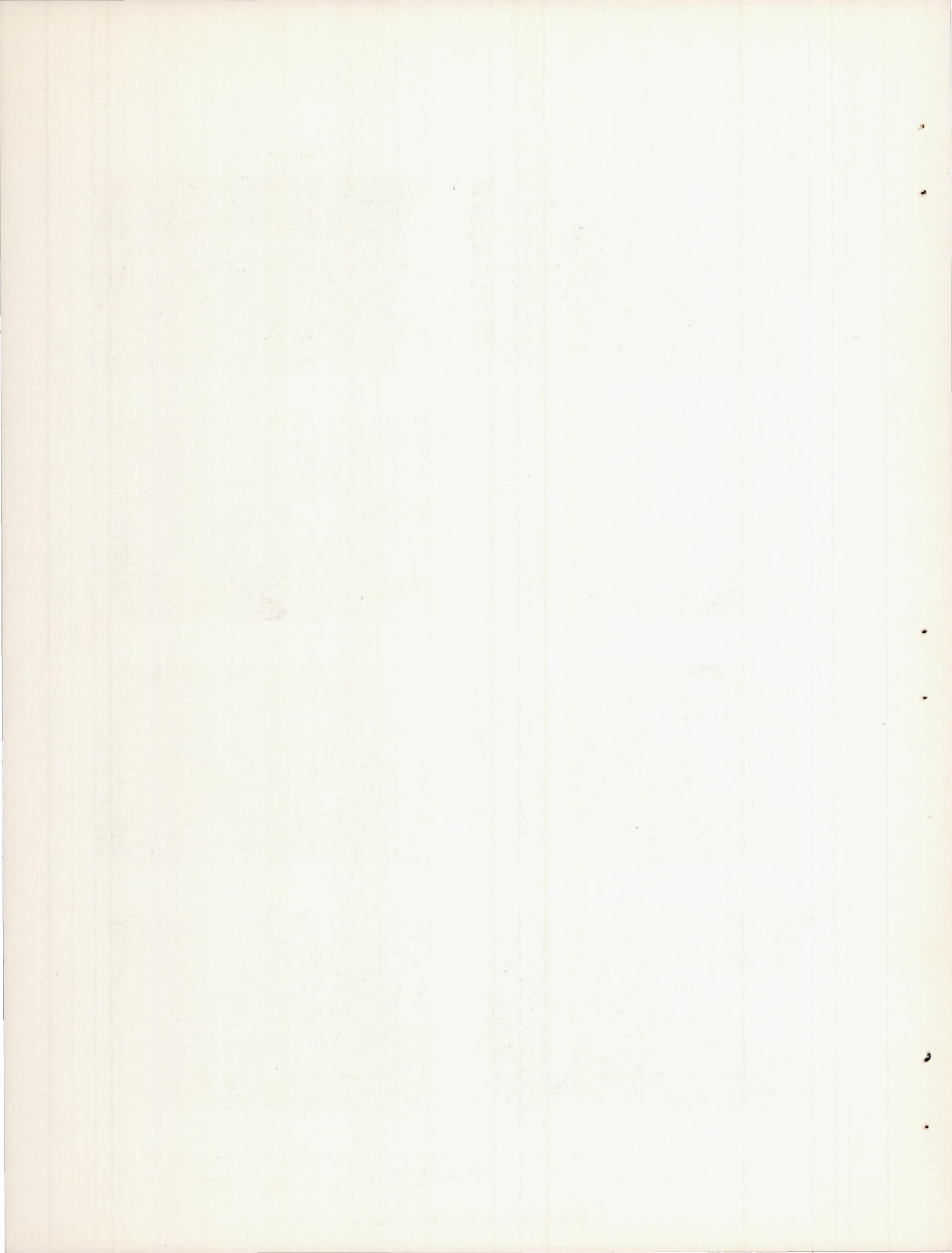
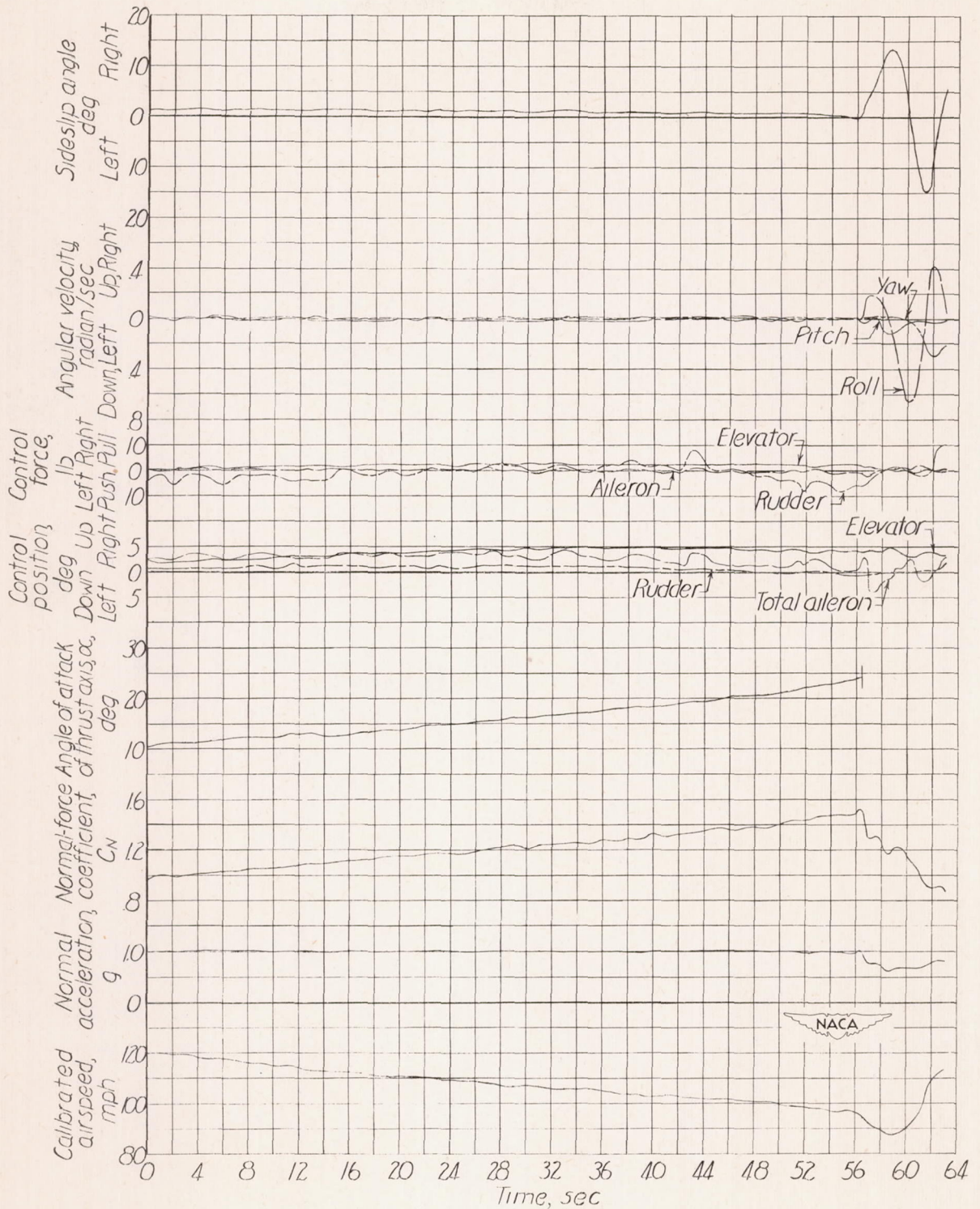


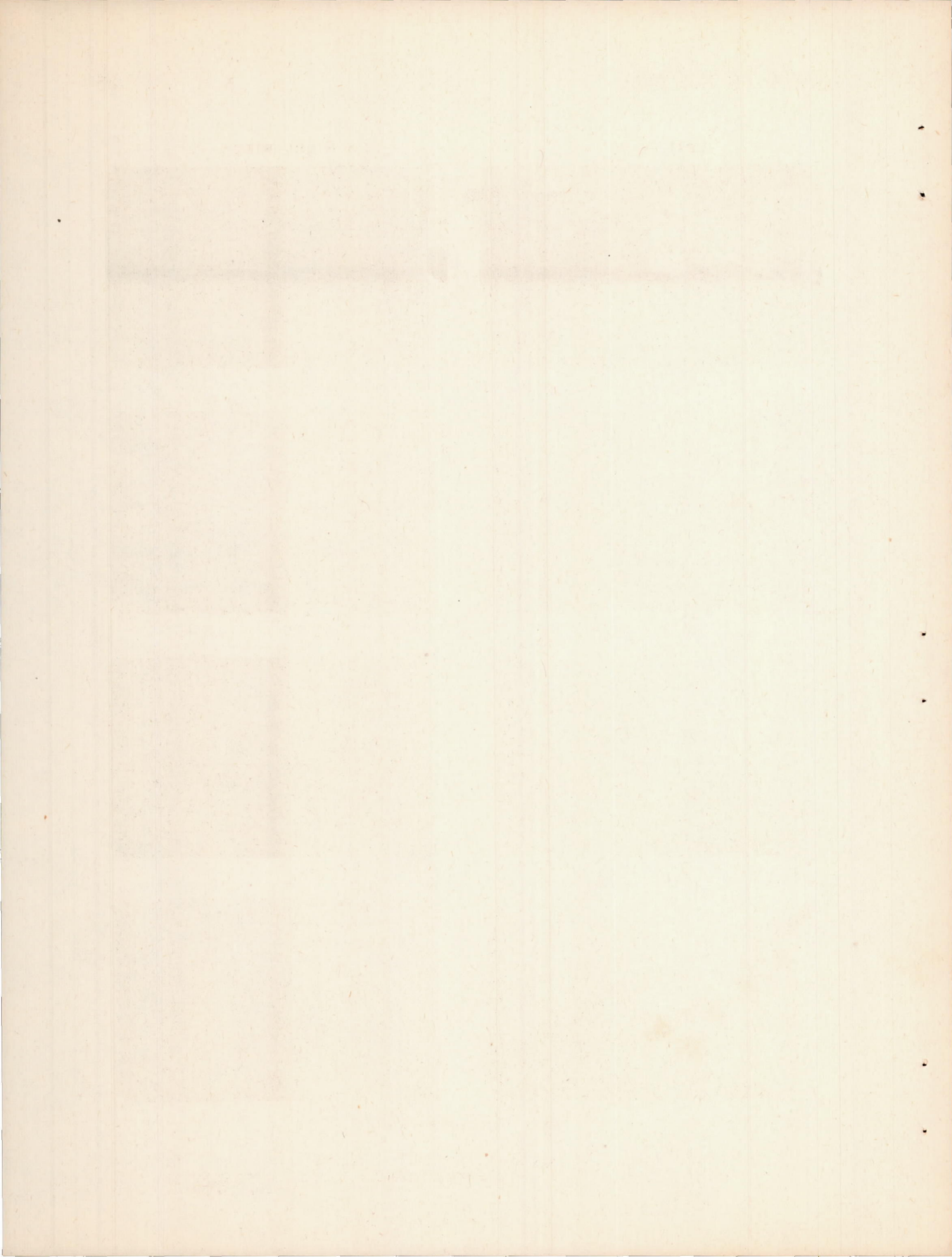
Figure 15.- Concluded.





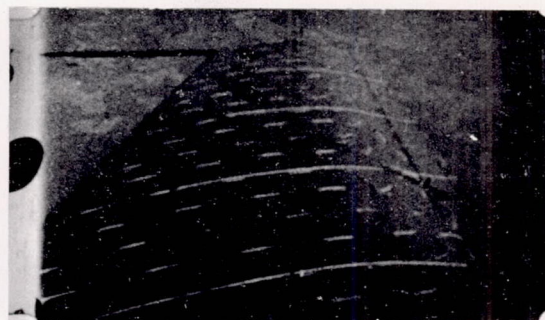
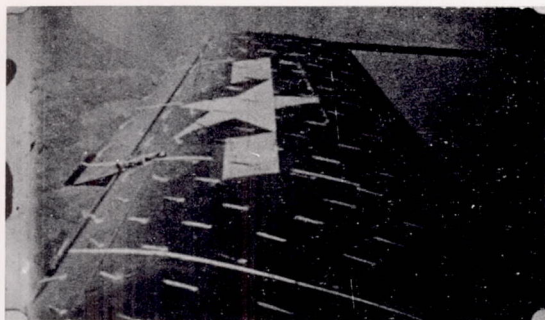
(a) Time history.

Figure 16.- Stall data for test airplane without slots on wing.
 Flaps down; nose wheel down; engine idling; center of gravity
 at 26.5 percent mean aerodynamic chord.

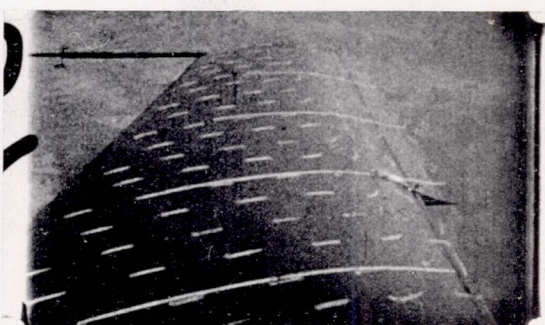
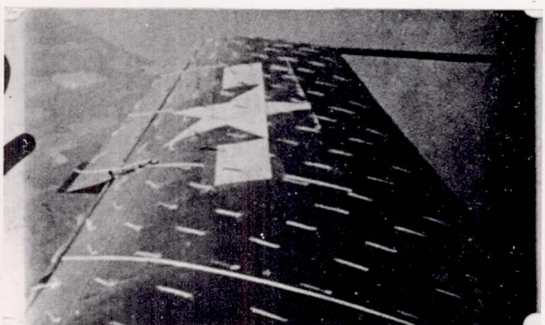


Left wing

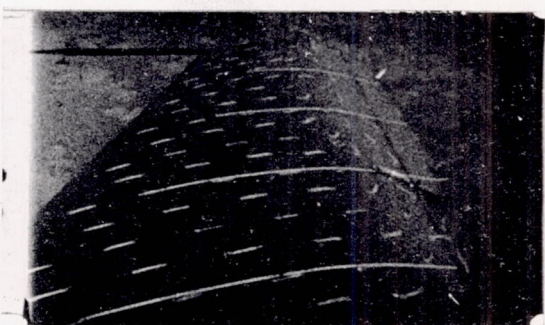
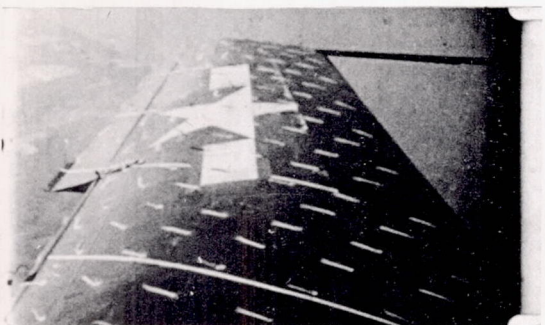
Right wing



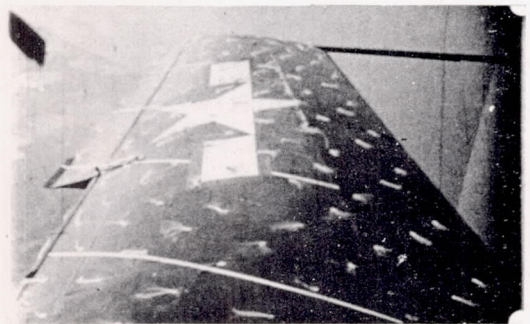
48.0 sec, $C_N = 1.38$, $\alpha = 20.5^\circ$



54.0 sec, $C_N = 1.47$, $\alpha = 22.8^\circ$



55.5 sec, $C_N = 1.48$, $\alpha = 23.6^\circ$



56.7 sec, $C_N = 1.39$

(b) Tuft pictures.

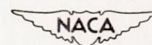
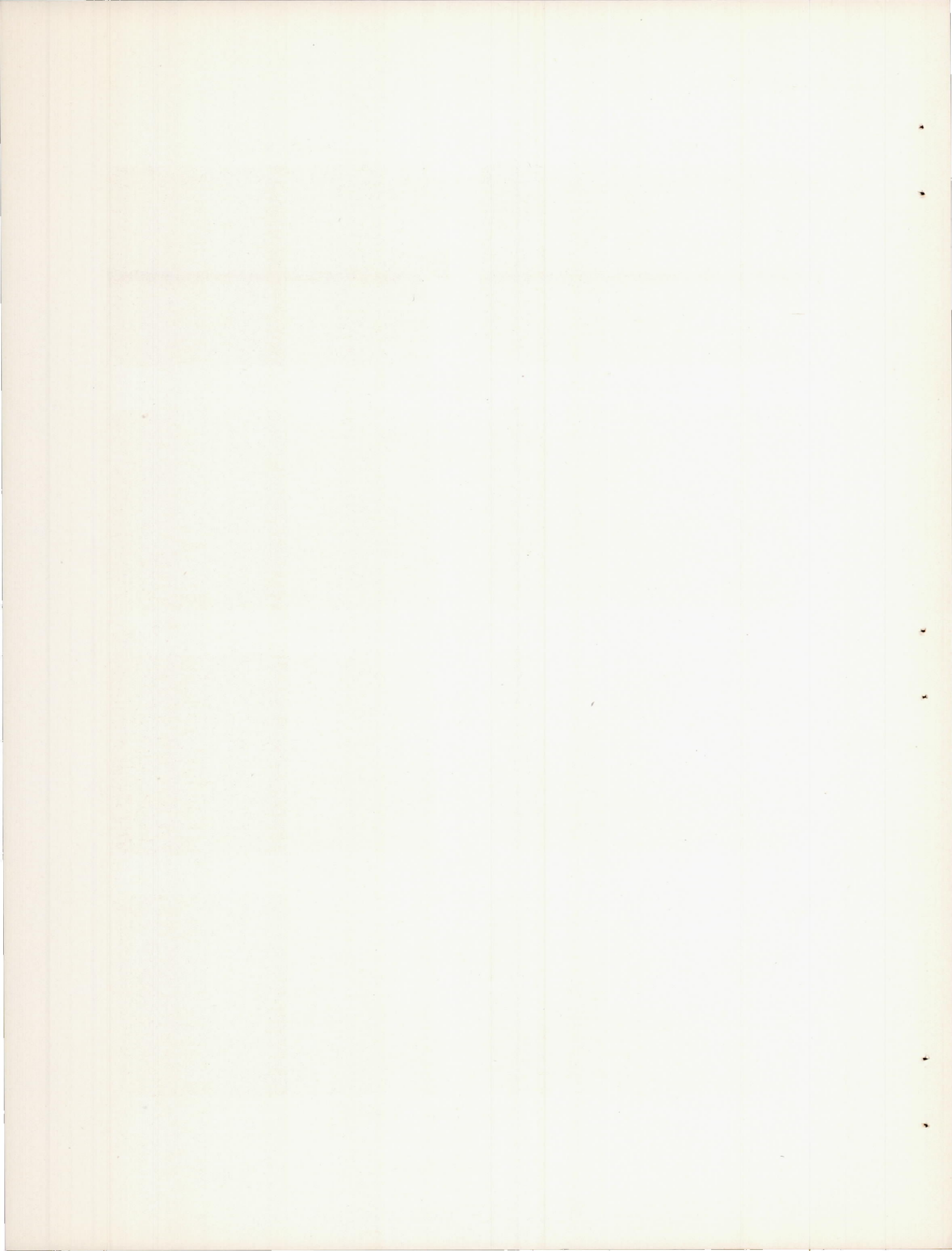
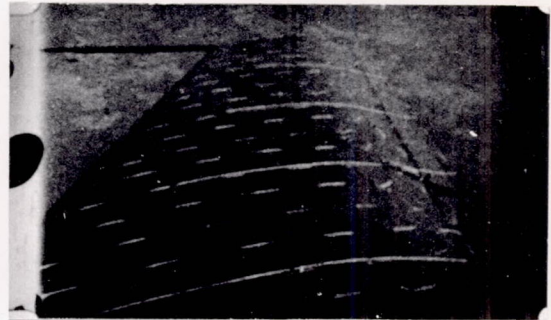
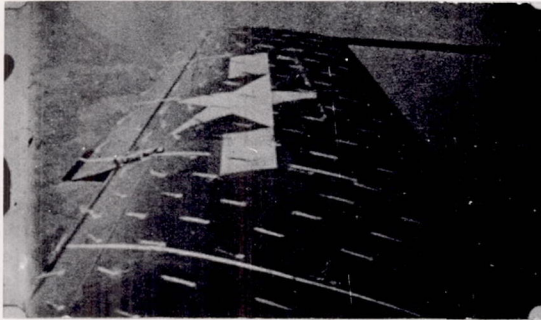


Figure 16.- Concluded.

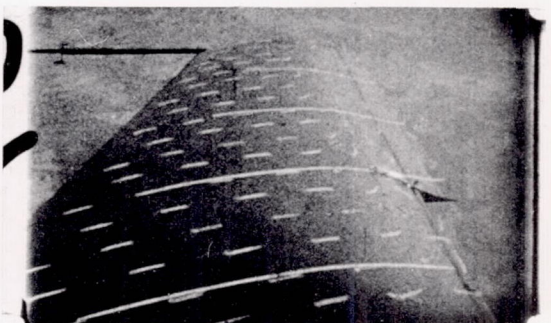
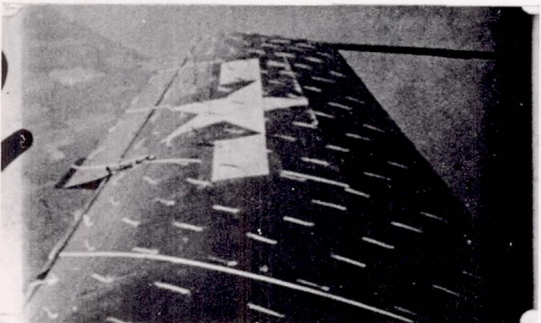


Left wing

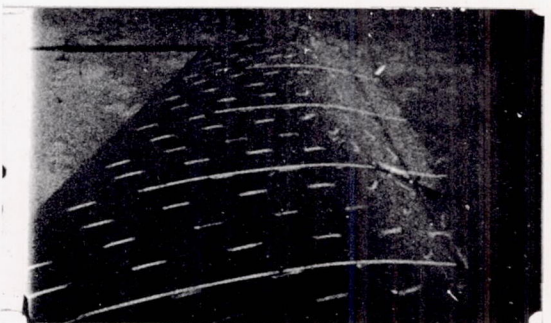
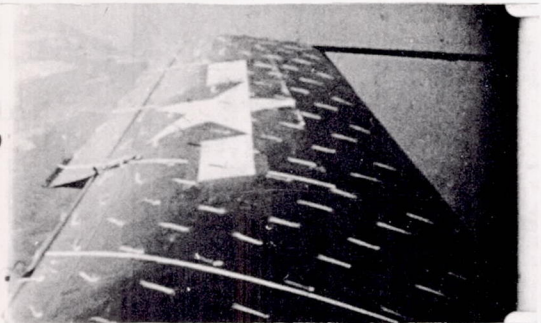
Right wing



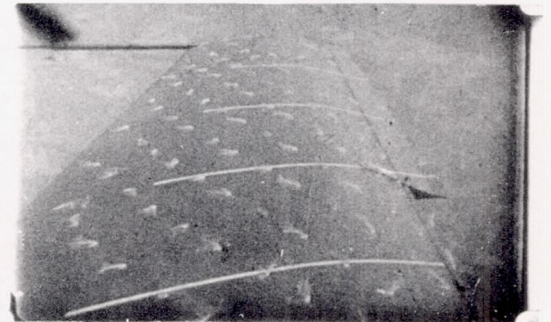
48.0 sec, $C_N = 1.38$, $\alpha = 20.5^\circ$



54.0 sec, $C_N = 1.47$, $\alpha = 22.8^\circ$



55.5 sec, $C_N = 1.48$, $\alpha = 23.6^\circ$



56.7 sec, $C_N = 1.39$

(b) Tuft pictures.

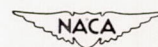
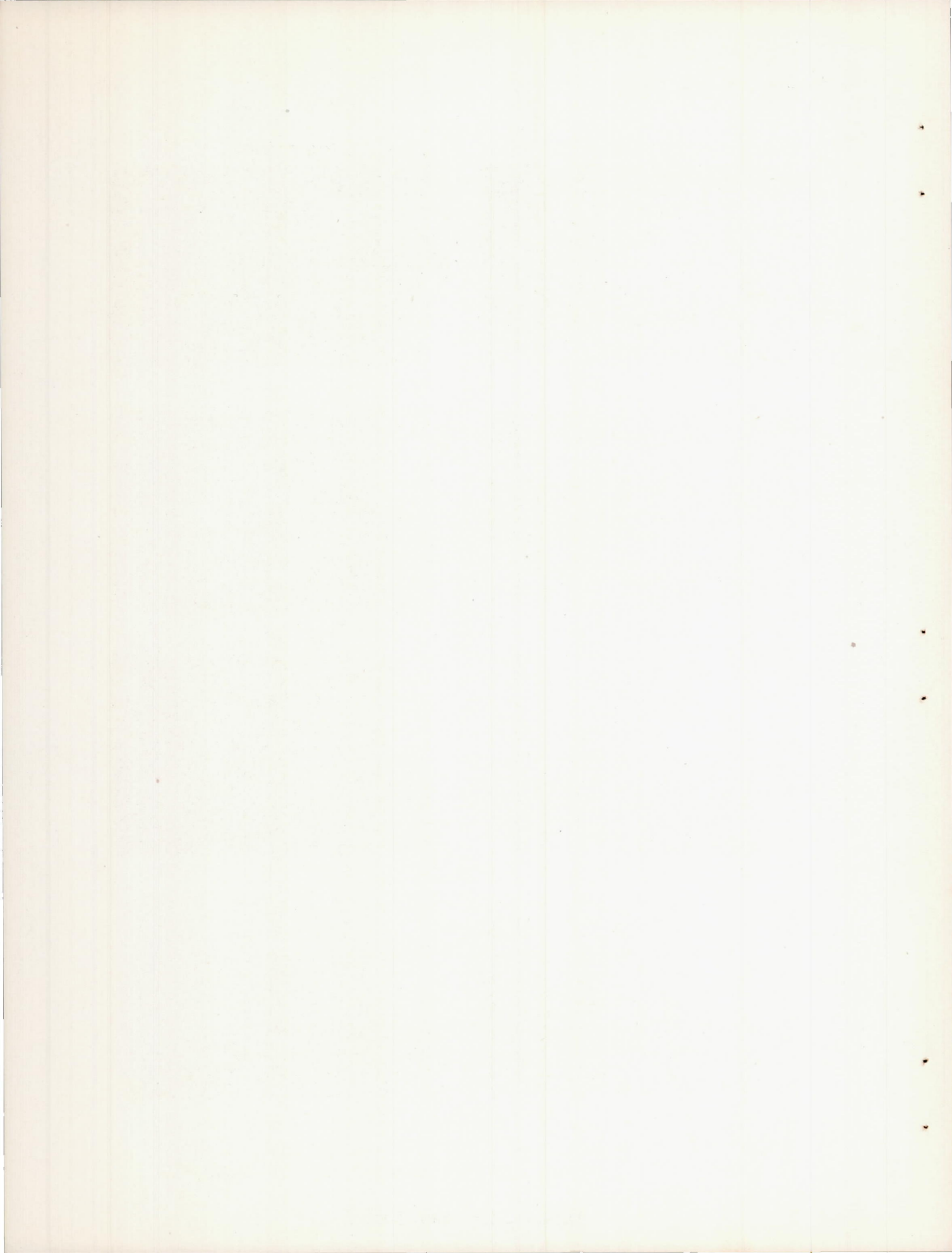


Figure 16.- Concluded.



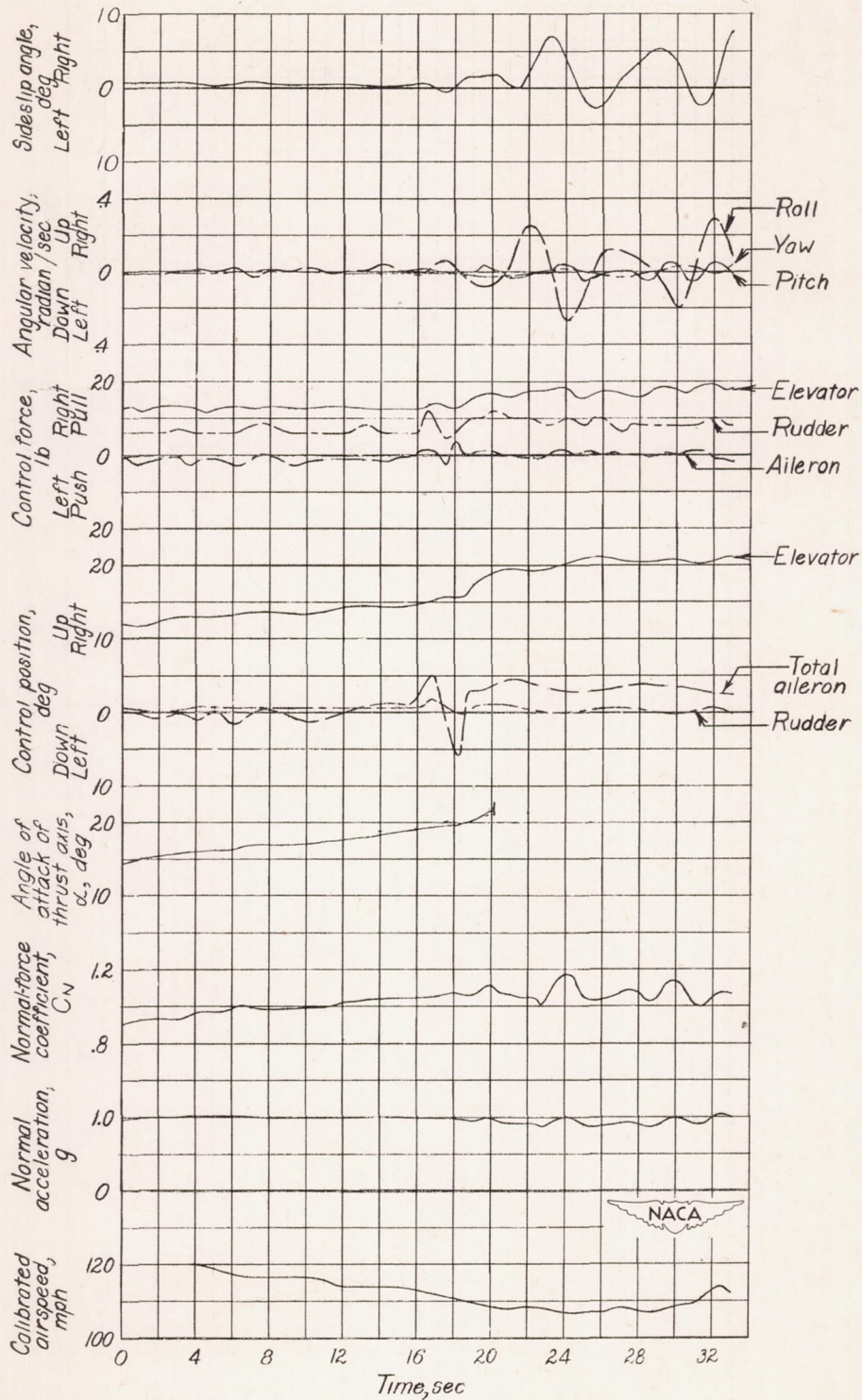


Figure 17.- Time history of stall for test airplane with 40-percent-span slots on wing. Flaps up; nose wheel up; engine idling; center of gravity at 20.7 percent mean aerodynamic chord.

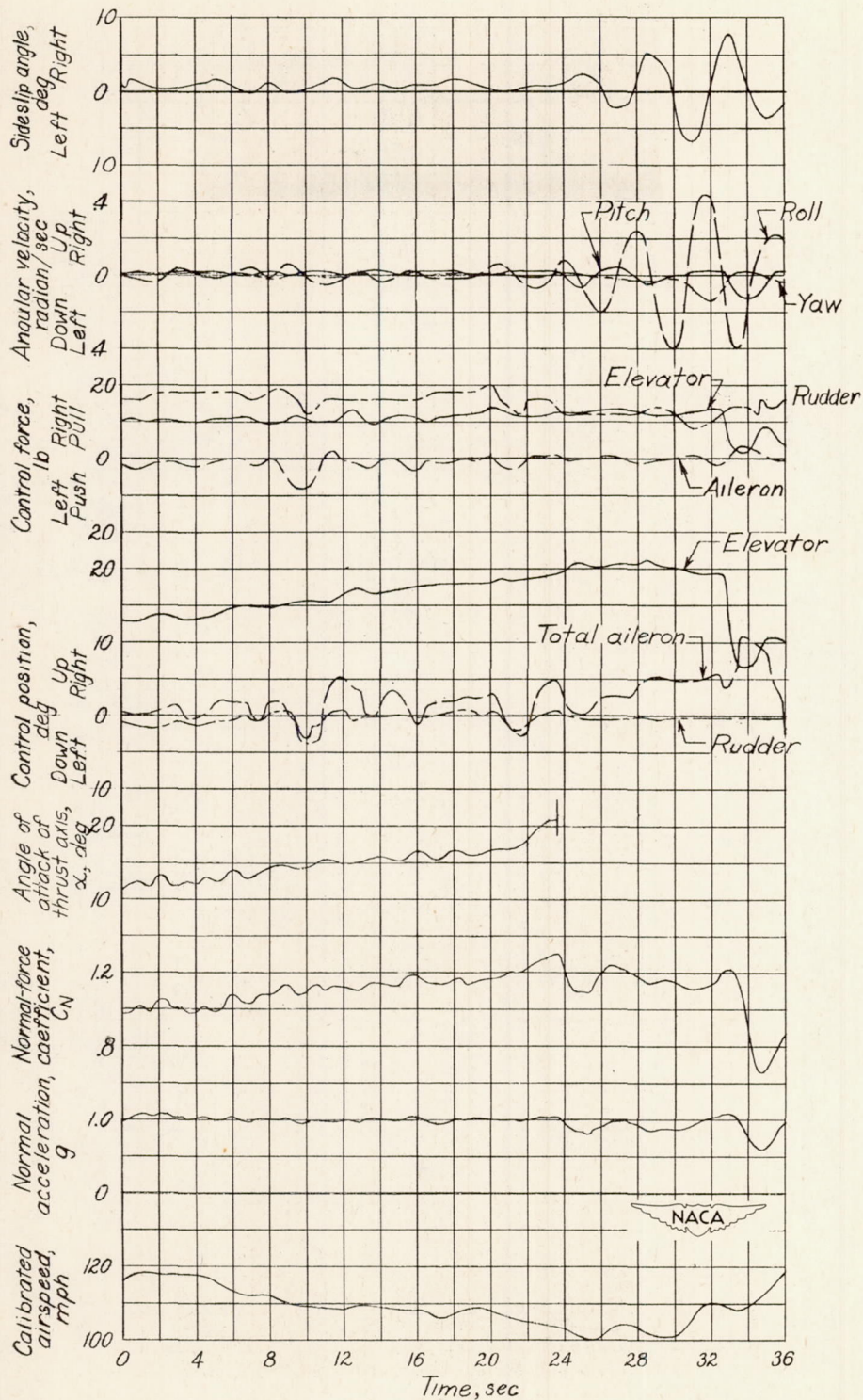
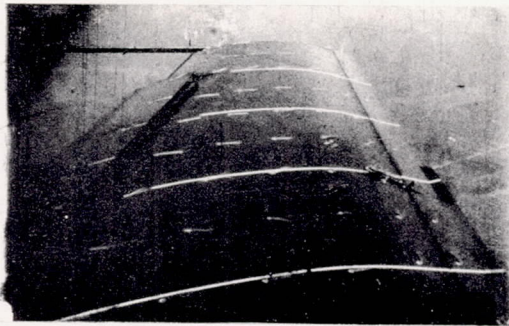


Figure 18.- Time history of stall for test airplane with 40-percent-span slots on wing. Flaps down; nose wheel down; engine idling; center of gravity at 20.3 percent mean aerodynamic chord.

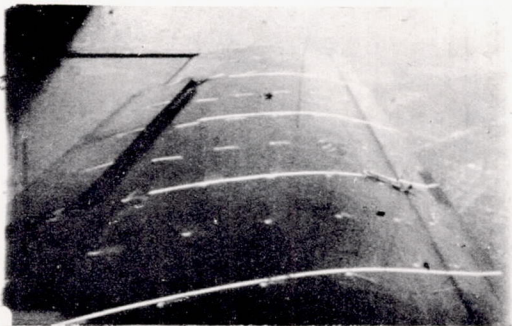
Right wing



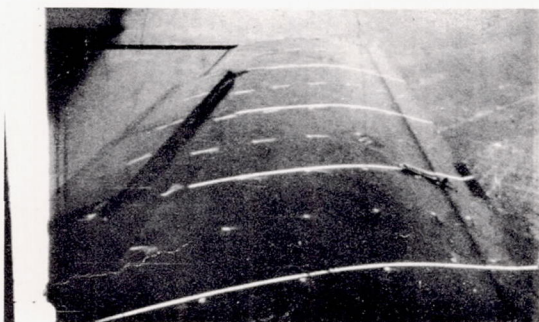
20.5 sec, $C_N = 1.06$, $\alpha = 17.5^\circ$



26.6 sec. $C_N = 1.11$, $\alpha = 18.5^\circ$

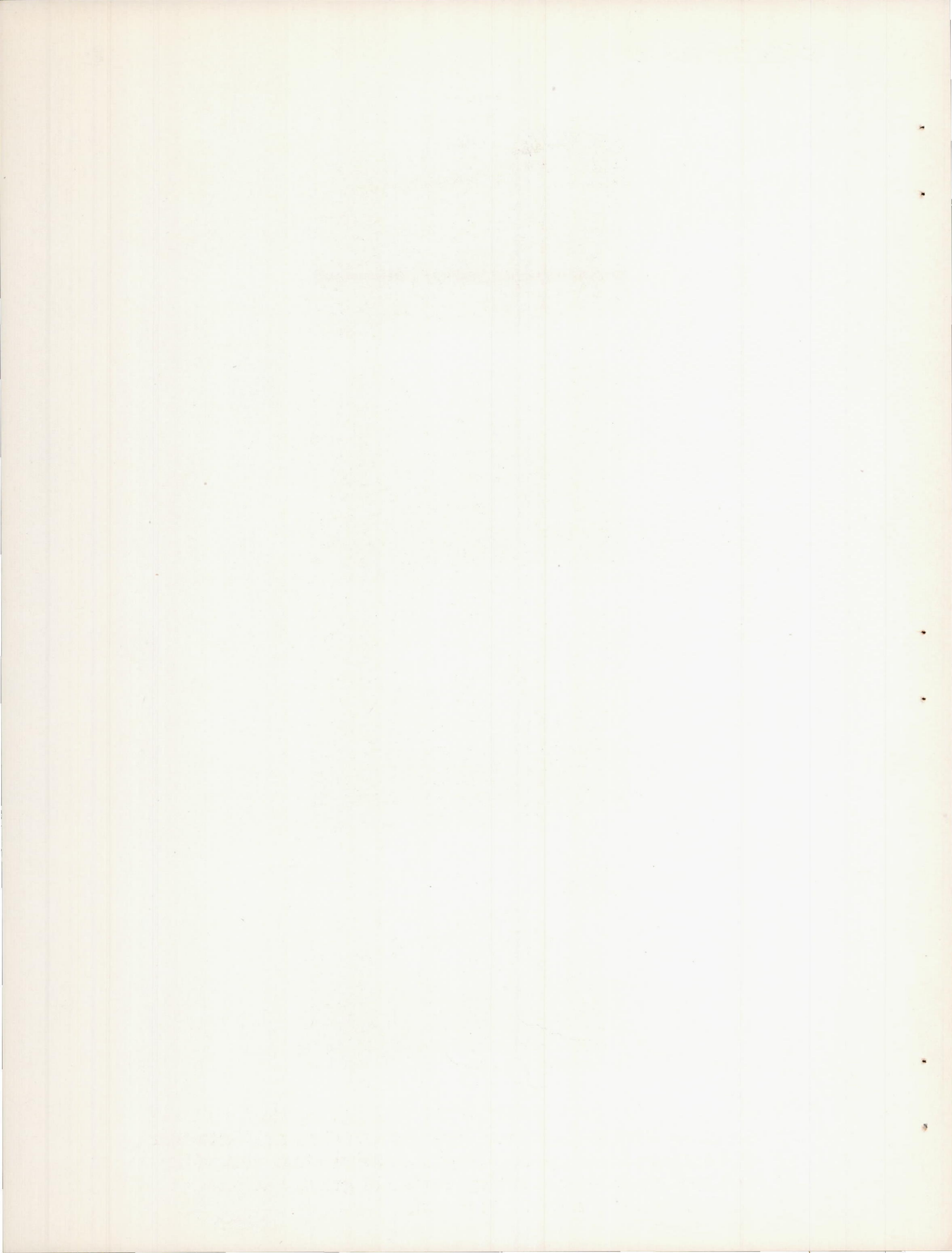


30.0 sec, $C_N = 1.13$, $\alpha = 19.0^\circ$



32.9 sec, $C_N = 1.15$

Figure 19.- Tuft pictures for right wing during stall with test airplane having 40-percent-span slots on wing. Flaps up; nose wheel up; engine idling; center of gravity at 26.4 percent mean aerodynamic chord.



Right wing

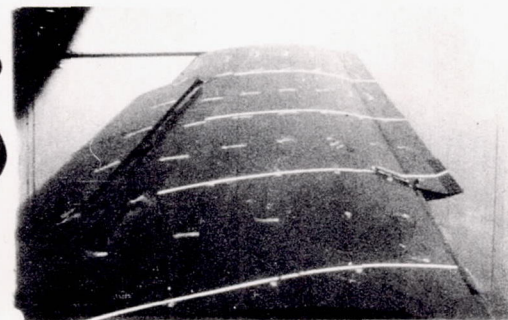
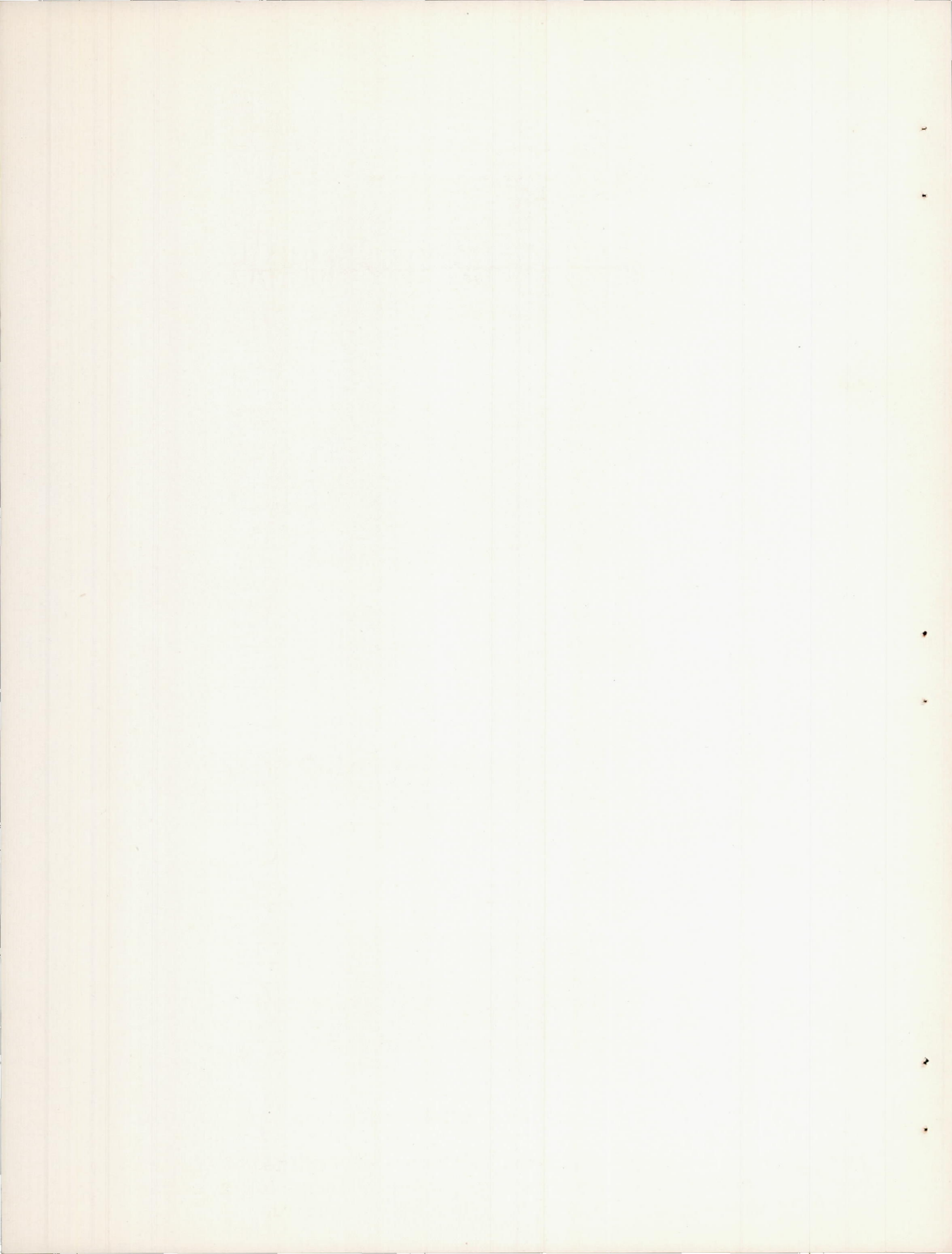
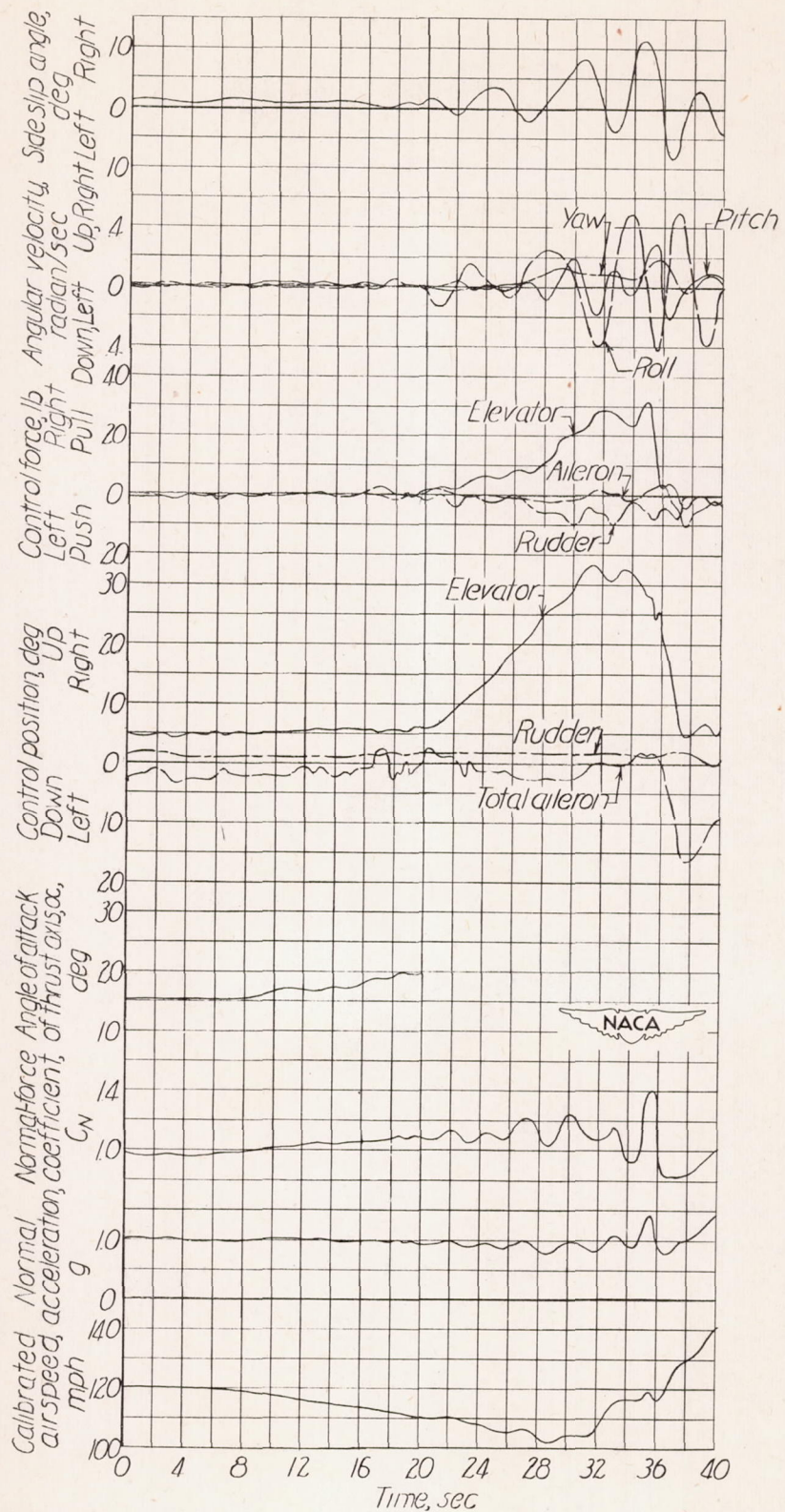
33.4 sec. $C_N = 1.24$, $\alpha = 17.1^\circ$ 39.0 sec. $C_N = 1.29$, $\alpha = 18.4^\circ$ 42.0 sec. $C_N = 1.30$, $\alpha = 19.6^\circ$ 45.0 sec. $C_N = 1.30$

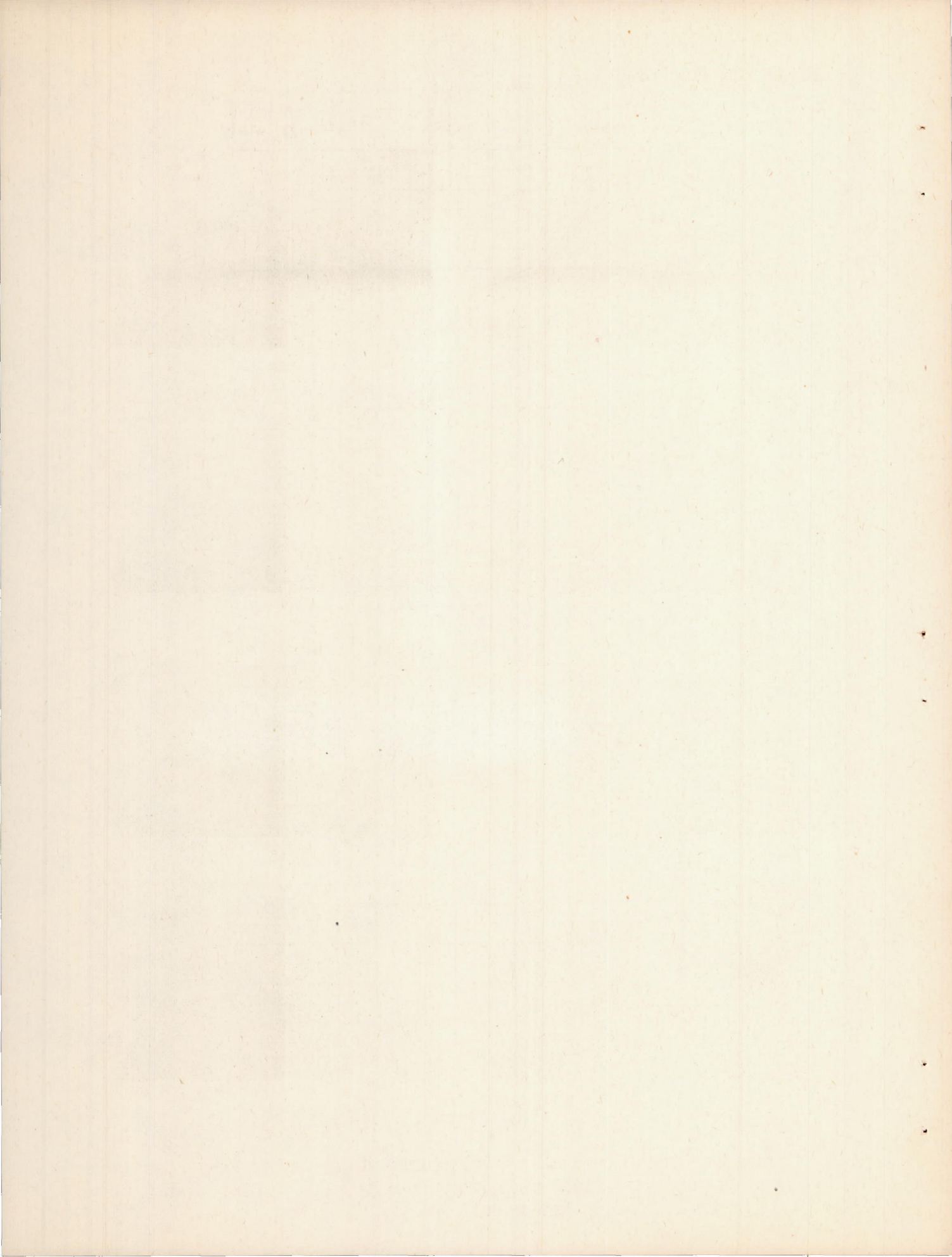
Figure 20.- Tuft pictures for right wing during stall with test airplane having 40-percent-span slots on wing. Flaps down; nose wheel down; engine idling; center of gravity at 26.4 percent mean aerodynamic chord.





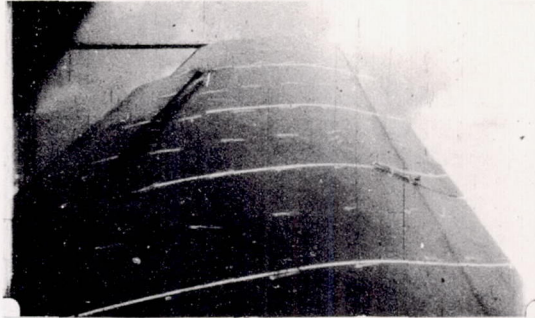
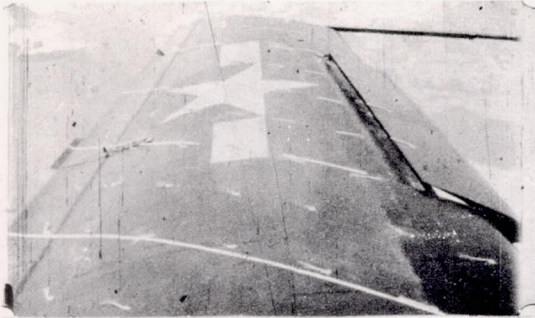
(a) Time history.

Figure 21.- Stall data for test airplane with modified 40-percent-span slots on wing. Flaps up; nose wheel up; engine idling; center of gravity at 26.4 percent mean aerodynamic chord.

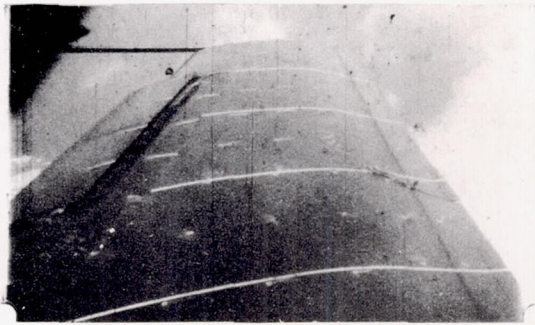
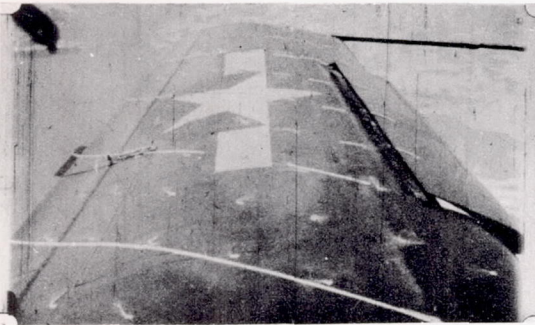


Left wing

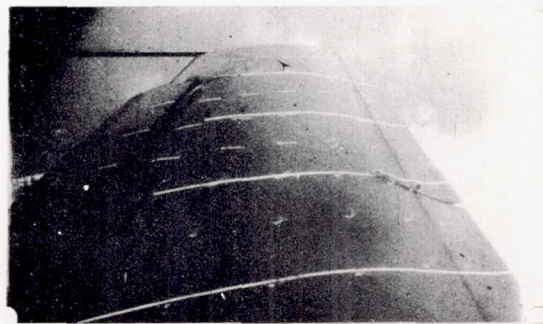
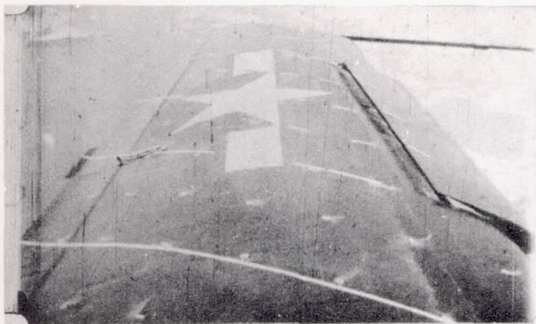
Right wing



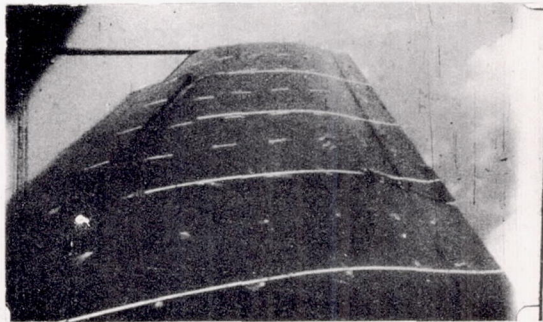
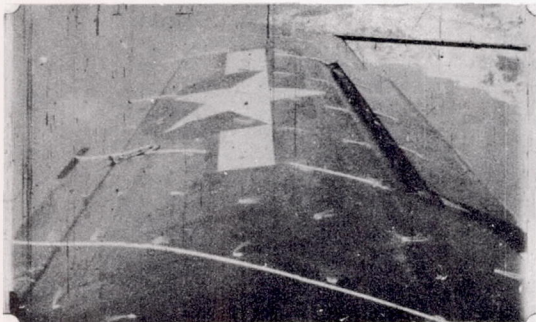
16.1 sec, $C_N = 1.06$, $\alpha = 18.1^\circ$



18.4 sec, $C_N = 1.09$, $\alpha = 19.6^\circ$



20.1 sec, $C_N = 1.08$, $\alpha = 19.5^\circ$



22.1 sec, $C_N = 1.13$

(b) Tuft pictures.

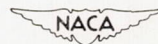
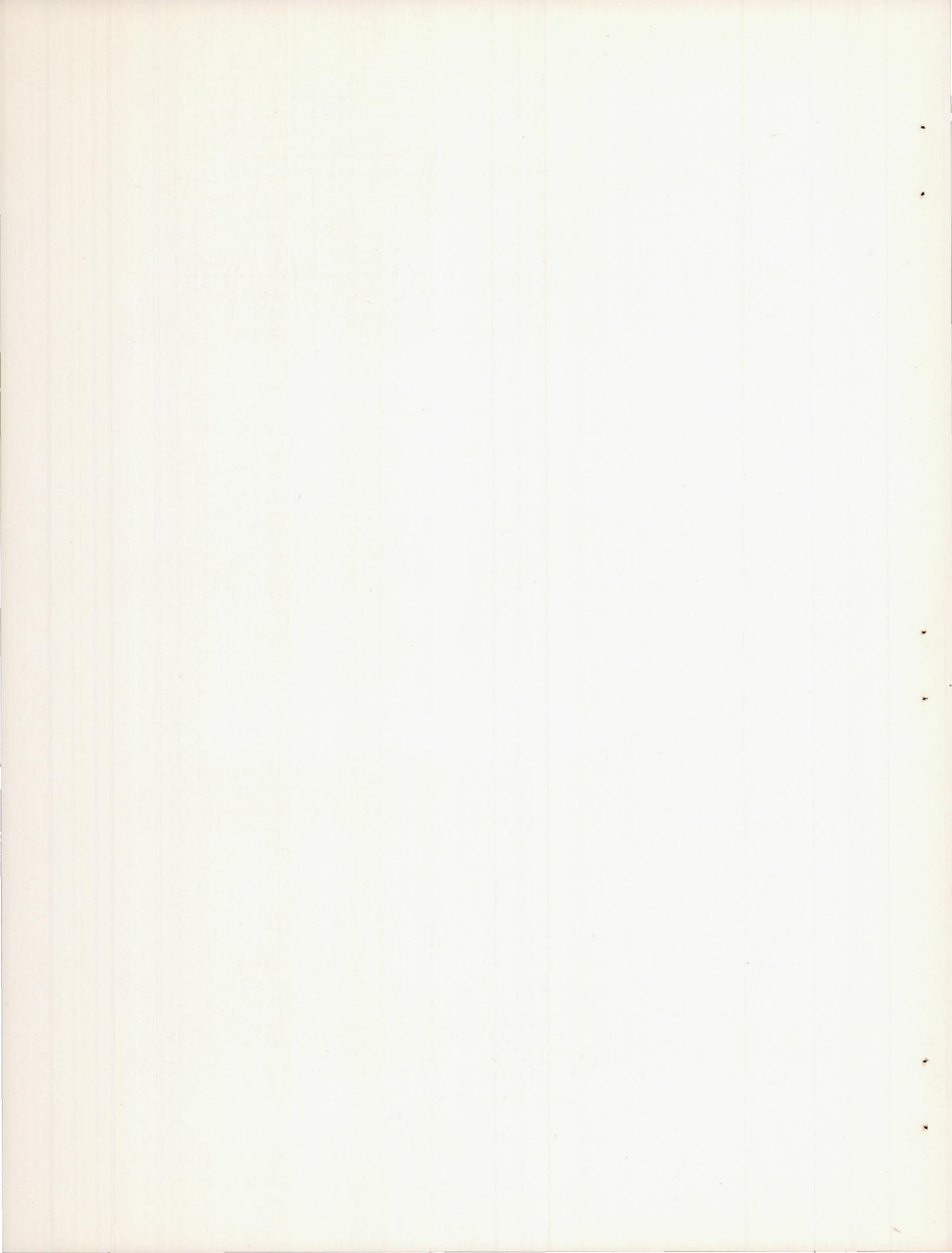
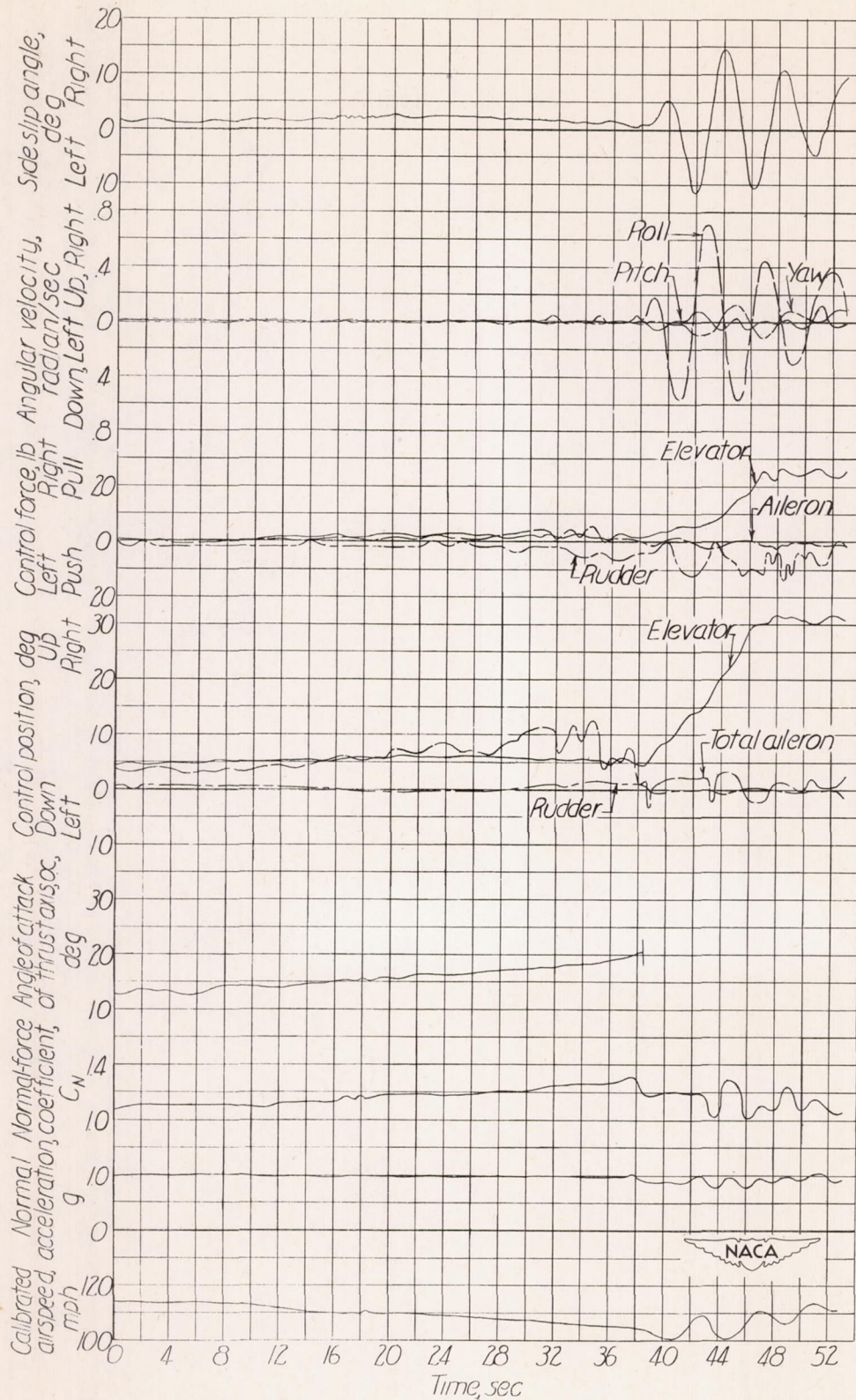


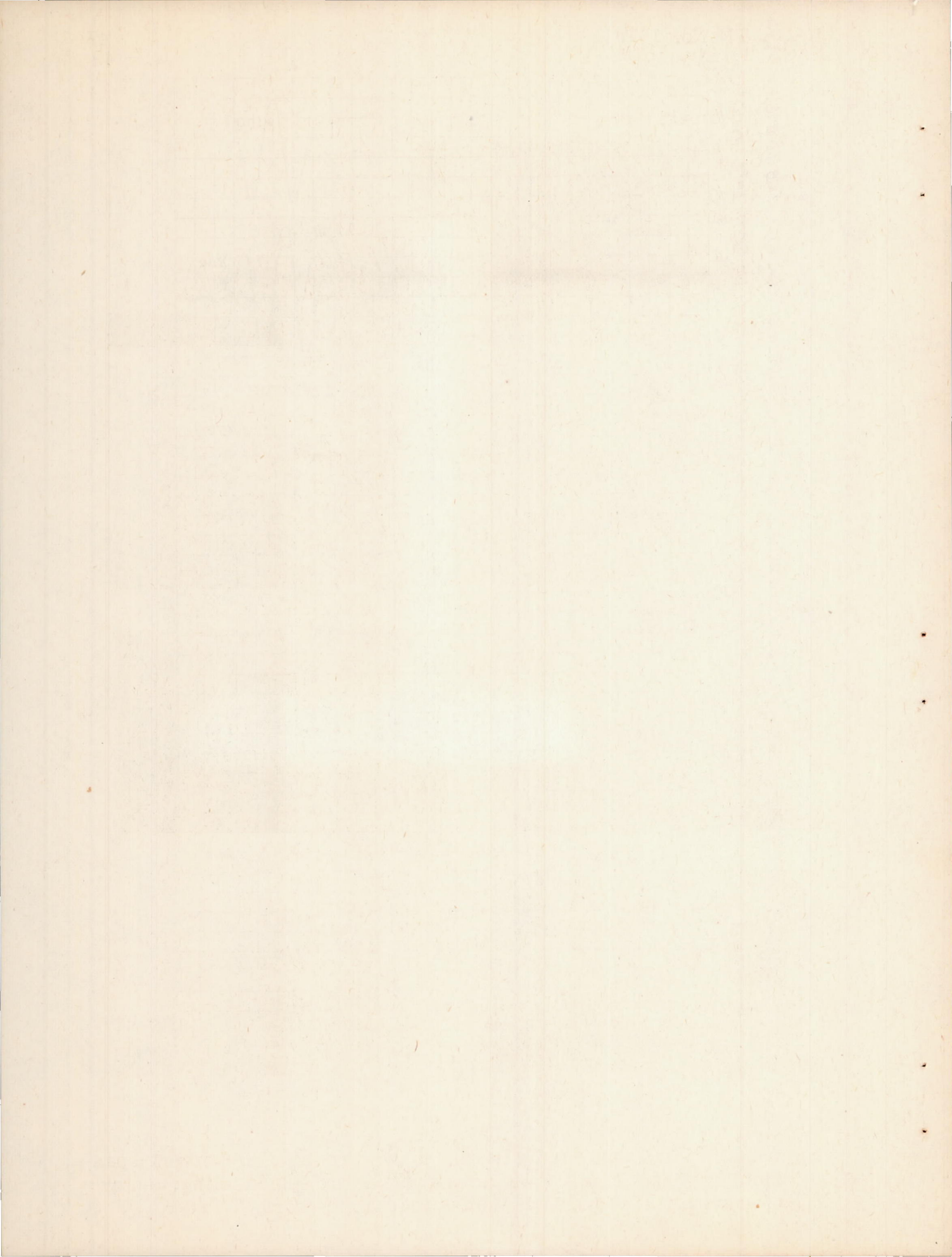
Figure 21.- Concluded.





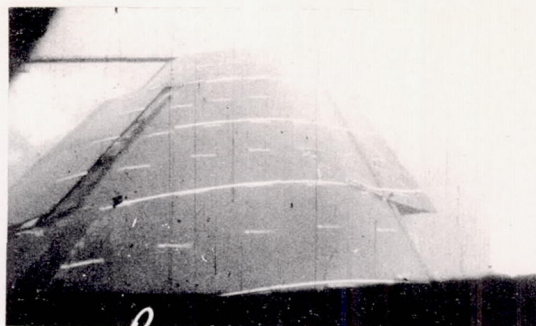
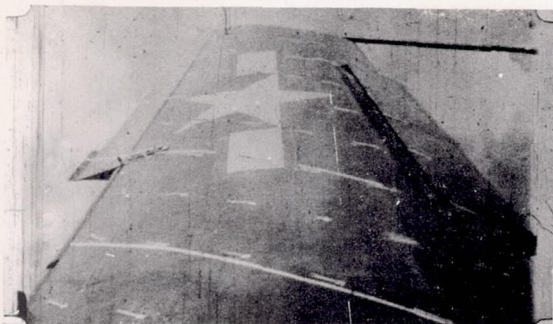
(a) Time history.

Figure 22.- Stall data for test airplane with modified 40-percent-span slots on wing. Flaps down; nose wheel down; engine idling; center of gravity at 27.1 percent mean aerodynamic chord.

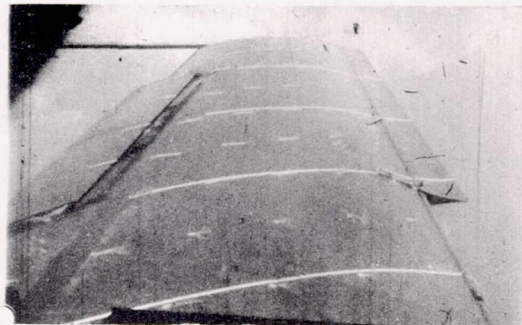
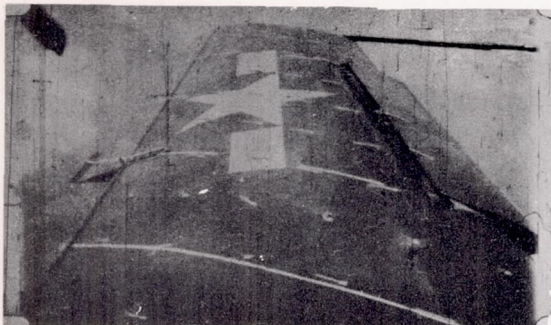


Left wing

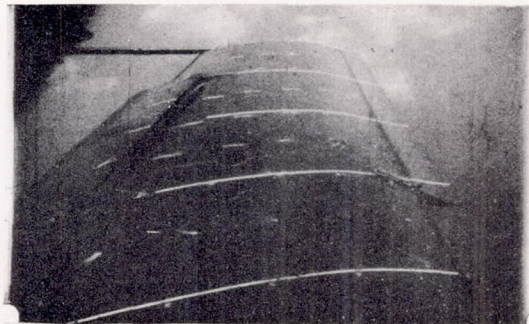
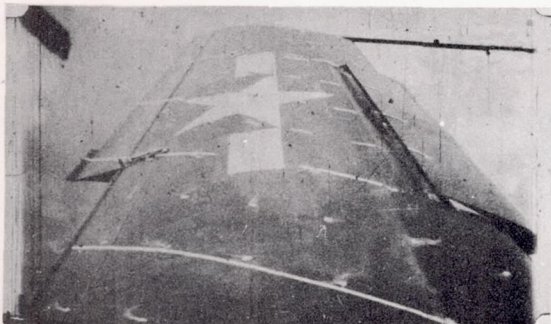
Right wing



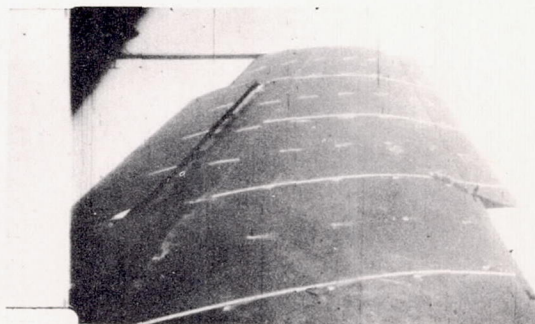
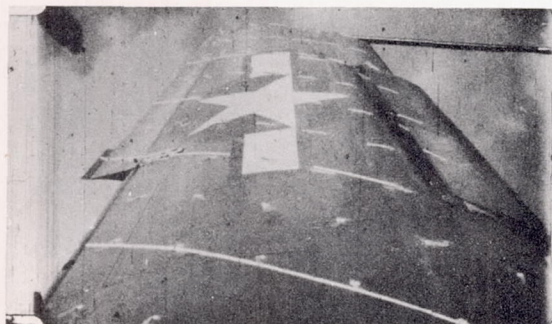
23.1 sec, $C_N = 1.18$, $\alpha = 16.3^\circ$



34.8 sec, $C_N = 1.26$, $\alpha = 18.3^\circ$



38.3 sec, $C_N = 1.22$, $\alpha = 20.5^\circ$



41.3 sec, $C_N = 1.19$

(b) Tuft pictures.

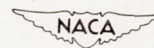
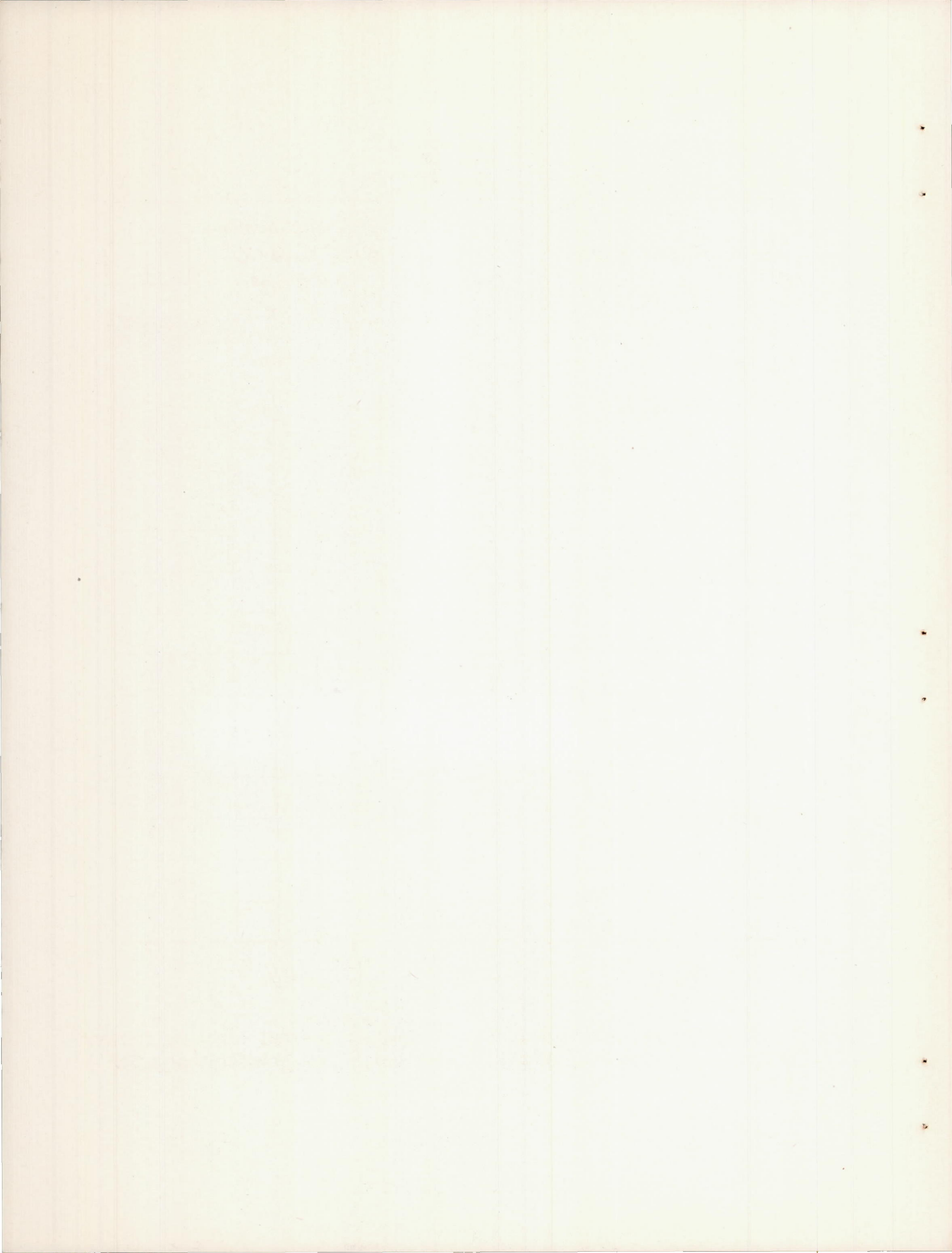


Figure 22.- Concluded.



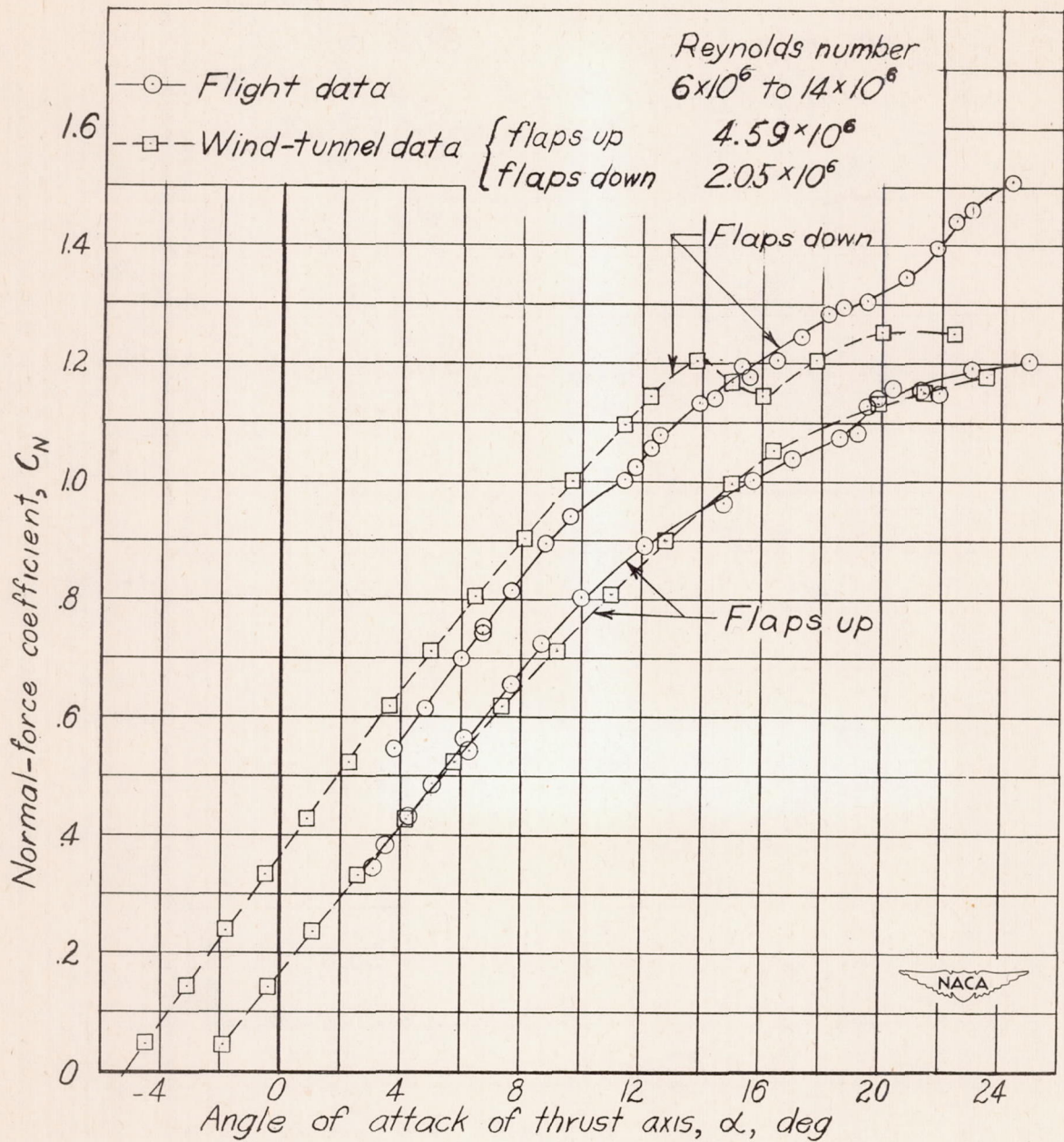


Figure 23.- Flight and wind-tunnel variation of normal-force coefficient with angle of attack of thrust axis for test airplane without slots on wing. Engine idling.

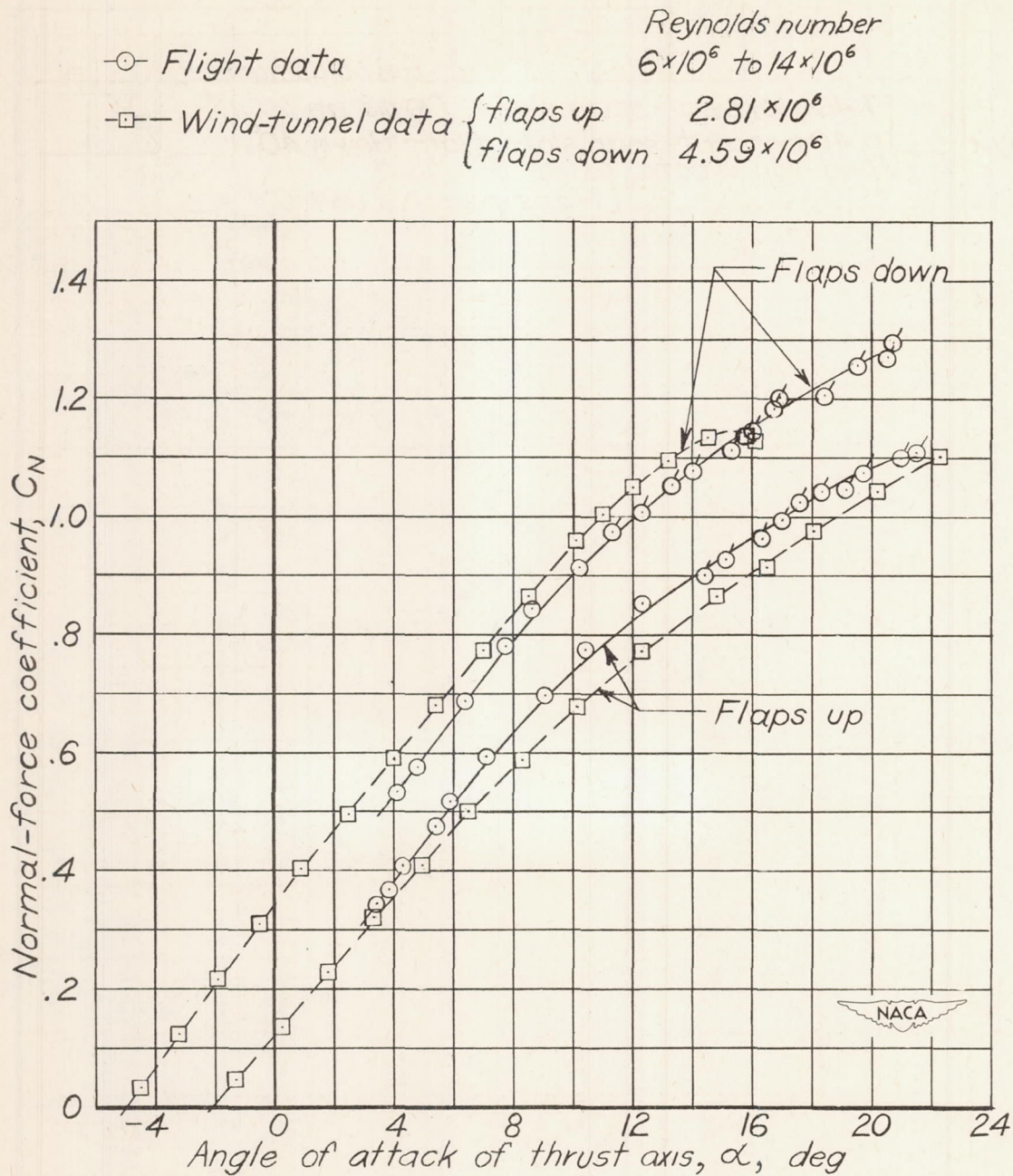


Figure 24.- Flight and wind-tunnel variation of normal-force coefficient with angle of attack of thrust axis for test airplane with 40-percent-span slots on wing. Engine idling.

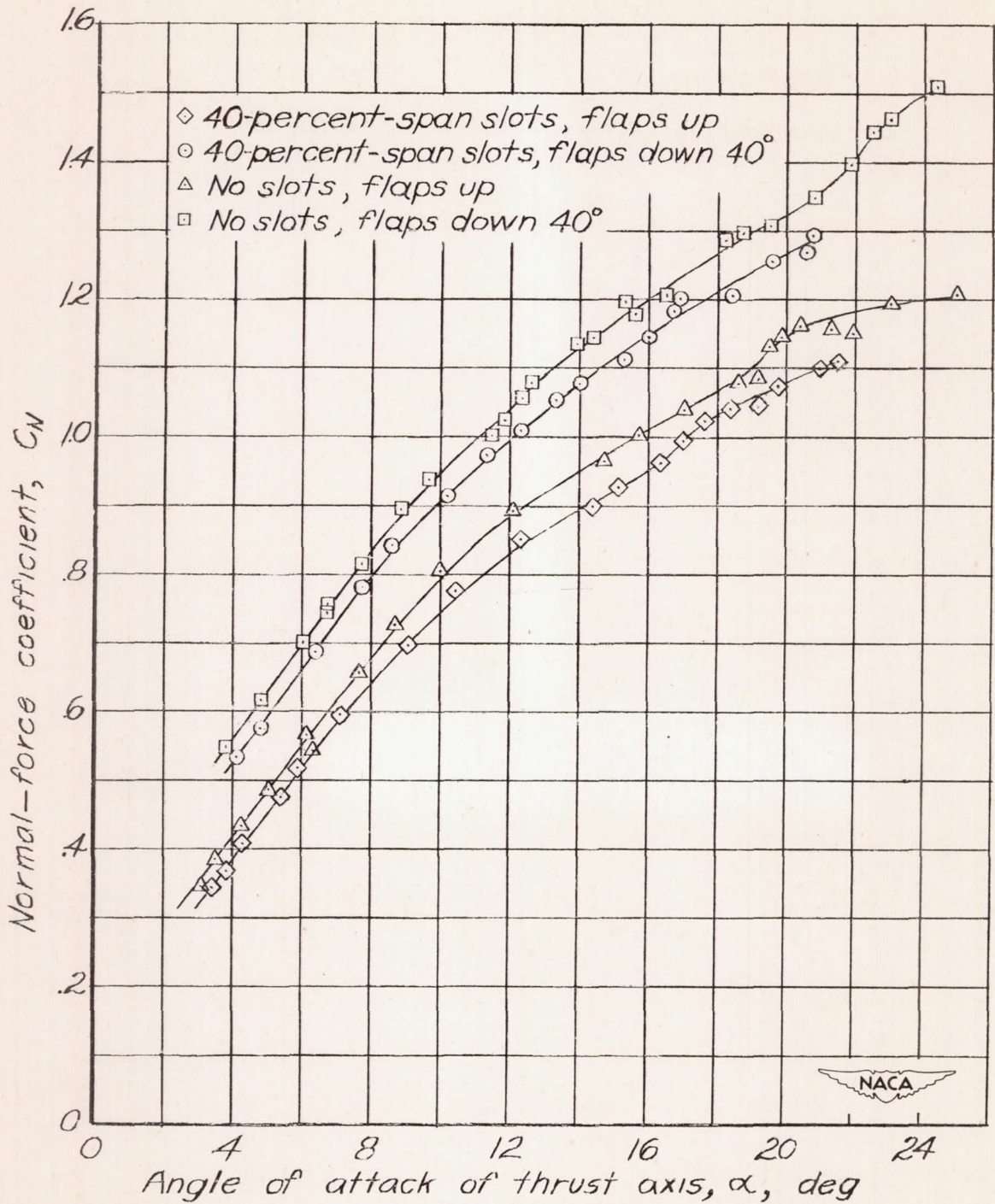


Figure 25.- Variation of normal-force coefficient with angle of attack of thrust axis for test airplane without slots and with 40-percent-span slots. Engine idling.

